GL02363

Senturion Sciences, Inc. • 1539 N. 105TH E. AVE. • P. O. BOX 15447 • TULSA, OKLAHOMA 74112 • (918) 836-6746

SOUTH DIXIE VALLEY, NEVADA

SCALAR MAGNETOTELLURIC SURVEY REPORT

Townships 22 North to 24 North
Ranges 33 East to 37 East
In Churchill County, Nevada

February 1978

Senturion Sciences, Inc., has performed the field work, analyzed the data and interpreted the results for this task. All the data and information resulting from this survey are the property of Southland Royalty Company.

SURVEY SPECIFICATIONS

LOCATION:	Dixie Valley, Nevada
AREA COVERED:	Approximately 20 square miles
ACQUISITION DATE:	November 1977 through January 1978
CREW:	Senturion Sciences #2
CODE:	South Dixie, 316
NUMBER OF STATIONS:	Scalar - 27 Tensor - 1
GEOPHYSICIST:	Will Czimer

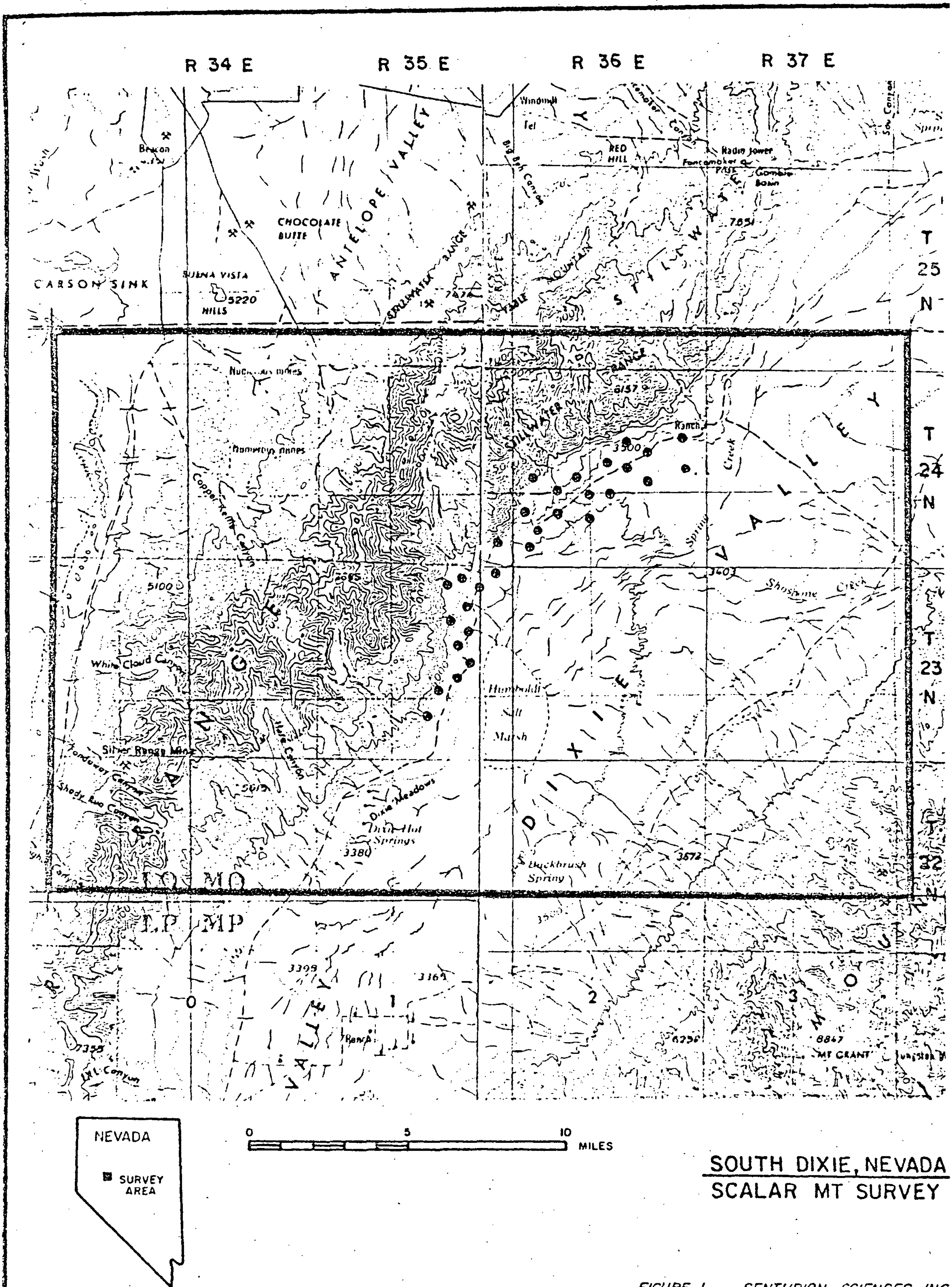

SOUTH DIXIE, NEVADA

SCALAR MT SURVEY

FIGURE 1 SENTURION SCIENCES, INC.

SOUTHLAND ROYALTY COMPANY'S

SOUTH DIXIE, NEVADA

SCALAR MAGNETOTELLURIC SURVEY REPORT

SUMMARY

The South Dixie Scalar Magnetotelluric survey (Figure 1) located the heat source and three successive shallower zones of high conductivity. These features are directly related to major faulting and abnormal gradients identified by the Dixie Valley MultiLevel Aeromagnetic survey (Features Map, Figure 2, Plate 1).

The areas with the greatest geothermal potential were interpreted as: the Stillwater anomaly (stations #9, #10 and #19), the Dixie Site anomaly (station #1) and the Mine anomaly (stations #17 and #30).

GEOLOGY

Dixie Valley and the contiguous Stillwater and Clan Alpine Mountains are in the western portion of the Basin and Range Province (Figure 3). According to Smith (1968), Dixie Valley is an asymmetrical composite graben intruded with a Middle Jurassic gabbroic lopolith. The average depth of alluvial and lacustrine valley fill is approximately 2500 feet. Tertiary and Jurassic andesite and basalt flows, tuffs, carbonates and gabbro are extensively exposed in the Stillwater Range and Clan Alpine Mountains. Earlier work for the client (Quigley, 1977) indicates high-angle reverse faulting along the eastern side of the Stillwater Mountains and thrusting from the east. Recent tectonic movement is evidenced by fault scarps from the 1954 earthquake and hot springs along the western edge of Dixie Valley.

MAGNETOTELLURIC INTERPRETATION

The South Dixie Magnetotelluric survey was composed of one tensor magnetotelluric (TMT) station which recorded three components of the magnetic field and two components of the telluric field, and 27 scalar magnetotelluric stations (SMT) which recorded one component of the telluric field. (One magnetic and orthogonal telluric field were, however, recorded at the scalar base station.) Analysis of the South Dixie Valley Aeromagnetic survey and available geology indicated a strong NNE strike direction. Scalar MT stations were therefore deployed to record at an azimuth of 22 degrees east of north, or the E-parallel telluric field.

Structural complexities prohibited utilization of the scalar base station sounding curve. Reduction of all scalar base station data indicated the base station was at some angle to the E-parallel orientation on the conductive side of a major lateral discontinuity. Senturion's TMT system with a three-component, Super-Conducting Quantum Interference Device (SQUID) was deployed in order to determine E-parallel and calculate the tensor impedances along the major axis of anisotropy (Figure 4). Normalized power spectra at the field stations were then multiplied by this sounding curve to yield the apparent resistivity versus period graph for each field station. Sounding curves, scalar survey procedures and MT techniques are listed in the Appendix.

MAGNETOTELLURIC RESULTS

The heat source (6 to 8 km) and three conductive anomalies were interpreted from the South Dixie MT survey. These results are in excellent agreement with features interpreted in the South Dixie Valley Aeromagnetic survey. The scalar-defined, near-surface heat sources correlated with areas along MultiLevel profiles which exhibited abnormal gradients. Several faulted scalar stations align with aeromagnetic-defined faults which probably provide the plumbing in the Dixie Valley geothermal system. Apparent resistivities at selected frequencies were plotted and contoured and are shown in Figure 5 and Figures 8 through 10 (also Plates 2-5). Conductive areas in these figures change location with respect to the frequency investigated. These variations are a function of depth and indicate changes in the complex plumbing patterns and/or rock porosity and permeability.

The apparent resistivity contour at five ohmmeters was chosen to correlate the 1-Hertz apparent resistivity of this survey (Figure 5) with AMT data (Figures 6 and 7) acquired by Senterfit, *et al* (1976). Excellent agreement exists between the two surveys, evidenced by the conductive anomaly (≤ 5 ohmmeters) overlap in T24N, R36E. Concerning the comparison between AMT and this survey data, the AMT field alignment was north to south and east to west. These orientations were 20 to 40 degrees from the true E-parallel; therefore, the AMT will not reflect true E-parallel apparent resistivities.

The 10-Second Apparent Resistivity Plat (Figure 8 and Plate 3) delineates a shift in the conductive anomaly southward from the Stillwater Mountains. Deeper penetration by the 10-second data suggests that the rock below the 1-Hertz conductive anomaly is becoming more resistive.

The 30-Second Apparent Resistivity Plat (Figure 9, Plate 4) reflects a slight northward trend in the conductive zones. This trend may be controlled by the high-angle reverse faulting on the eastern side of the Stillwater Mountain fault block (Quigley, 1977).

At 100-second period (Figure 10, Plate 5) the anomalously conductive areas are centered around a three-station anomaly to the north (stations #9, #10 and #19) and station #1 and perhaps #2 to the south. The northern anomaly coincides with an abnormal gradient identified on MultiLevel Profile A-A'. Scalar stations within the abnormal gradient of Profile E-E' exhibit conductivity to a slightly lesser degree than stations #9, #10 and #19. No MultiLevel information exists over stations #1 and #2.

Figures 11 and 12 illustrate results from one-dimensional modeling of the South Dixie SMT data. The isopach from the surface to resistive gabbroic complex averages approximately 2000 feet. This thickness correlates with MultiLevel depth calculations along the western side of Dixie

Valley. The surface to conductive half-space isopach indicates the conductive half-space ranged from depths of 6 to 14 km. Recent work by Stanley, *et al* (1977) revealed a highly conductive zone at depths that ranged from 18 km in the central part of the eastern Snake River Plain to 7 km beneath the Raft River thermal area, and as little as 5 km in Yellowstone. The near-surface South Dixie heat source anomalies (6 to 8 km depths) are believed to be significant to the geothermal potential of Dixie Valley. MultiLevel aeromagnetics support the existence of two shallow heat sources in T24N, R36E with abnormal gradients in Profiles A-A' and E-E'. Scalar MT data does not, however, support the extension of the abnormal gradient from Profile A to E (e.g., the depth to the conductive half-space at stations #12 and #20 was modeled at 12 km). The third shallow heat source is located at the South Dixie base station. This anomaly plunges to depths of 10 to 14 km beneath the closest MultiLevel profile (C-C') located 3/4 of a mile to the south of station #1.

CONCLUSIONS

The heat source in the South Dixie area and three conductive anomalies with the greatest geothermal potential are listed on the Features Map, Figure 2 and Plate 1. A heat source is defined as having anomalously low resistivity (1 to 5 ohmmeters) at depths from 6 to 8 km. The conductive anomalies are defined as having apparent resistivities $\leq$ 20 ohmmeters at the 30-second period.

Scalar MT data suggests the heat source rises to within 6 to 8 km of the surface at three locations. Two of these areas in T24N, R36E correlate with abnormal gradients in the Dixie Valley MultiLevel Aeromagnetic survey. Furthermore, modeling of the SMT data suggests these two areas are separate since the conductive half-space plunges to depths of 12 km between the MultiLevel Profiles A-A' and E-E' at stations #12 and #20. No MultiLevel data exists over the third anomalous area at station #1.

The Stillwater, Dixie Site and Mine anomalies appear to be directly associated with the heat source anomalies, fault zones and structural trends identified by the MT and aeromagnetic surveys. The Stillwater anomaly consists of four stations, three of which delineated the shallow heat source at the southwestern corner of T24N, R36E. This anomaly is at the confluence of several faults which apparently provide the plumbing for migrating fluids from the heat source.

The Dixie Site anomaly between the Old Stillwater and Marsh faults includes two stations. Station #1 locates another heat source, and station #2 is faulted by the possible southern extension of the northern branch of the Old Stillwater fault or perhaps by a shear zone which offsets the Old Stillwater faults.

The Mine anomaly consists of two stations (#17 and #30) and is associated with the heat source located in the center of T24N, R36E. The Mud, Stillwater Thrust and station #14 faults could plumb this anomaly.

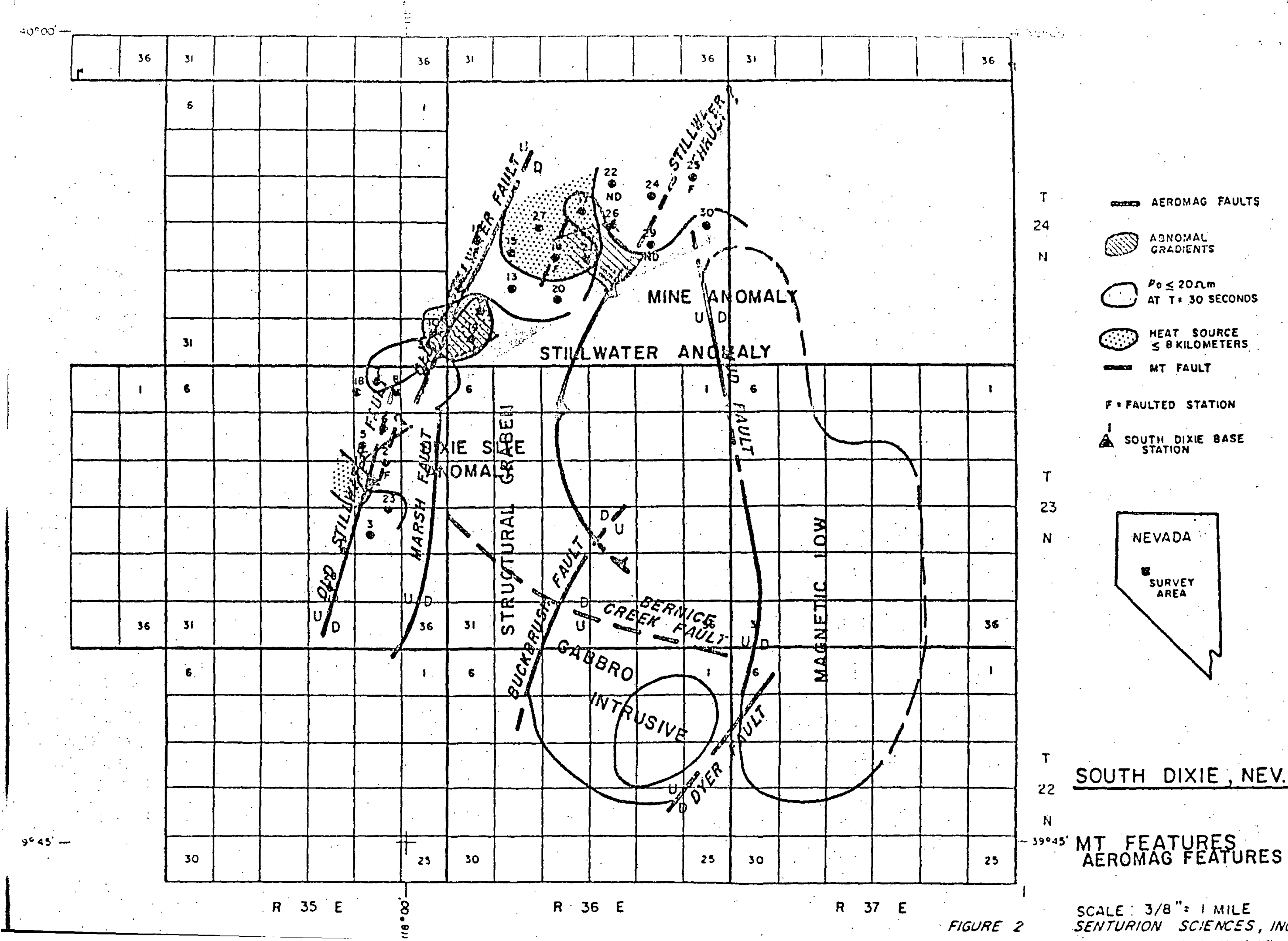

SOUTH DIXIE, NEV.

MT FEATURES
AEROMAG FEATURES

SCALE: 3/8" = 1 MILE

FIGURE 2

SENTURION SCIENCES, INC

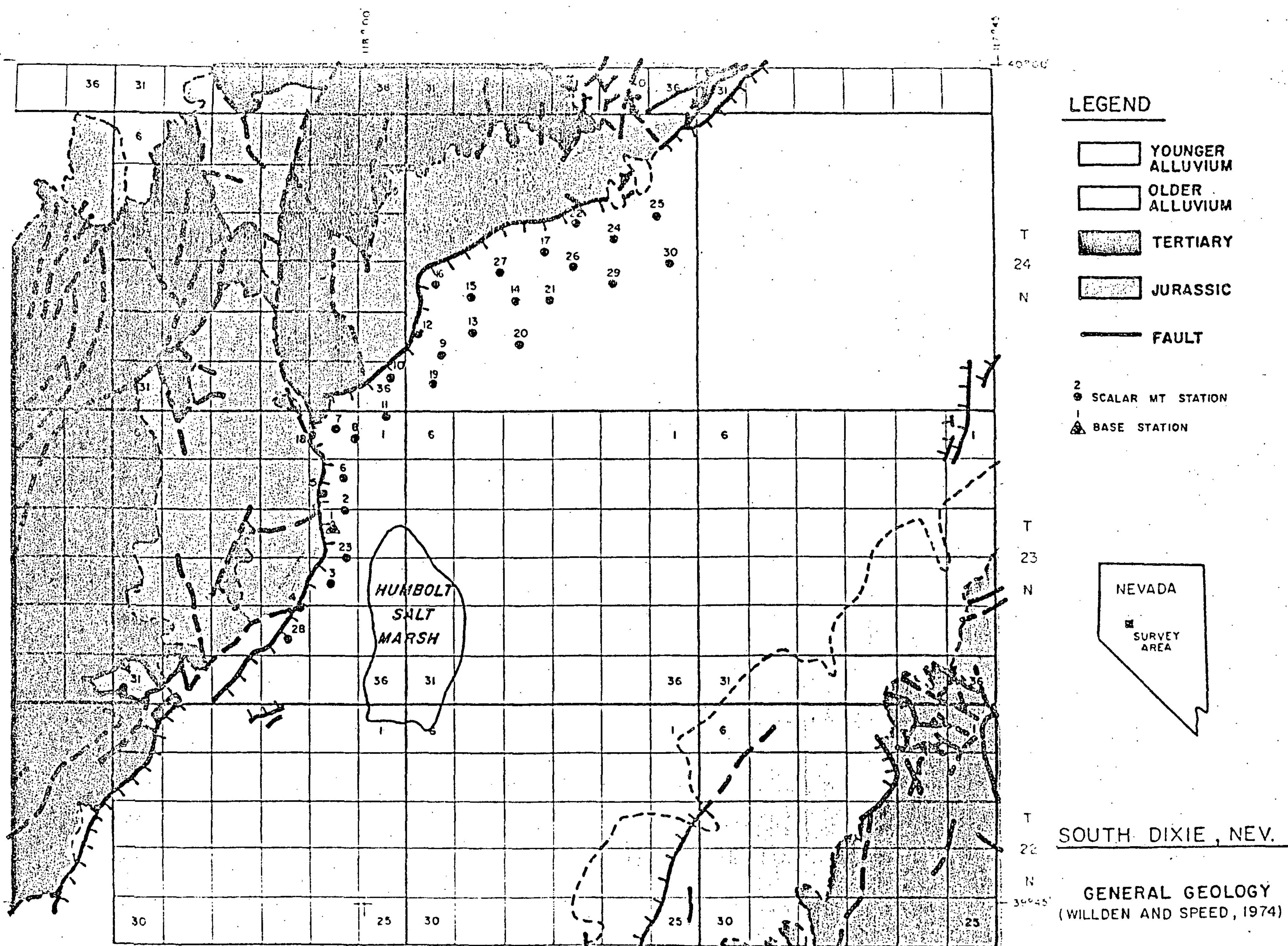

SOUTH DIXIE, NEV.

GENERAL GEOLOGY
(WILLDEN AND SPEED, 1974)

SCALE: 3/8" = 1 MILE
SENTURION SCIENCES, INC.

FIGURE 3

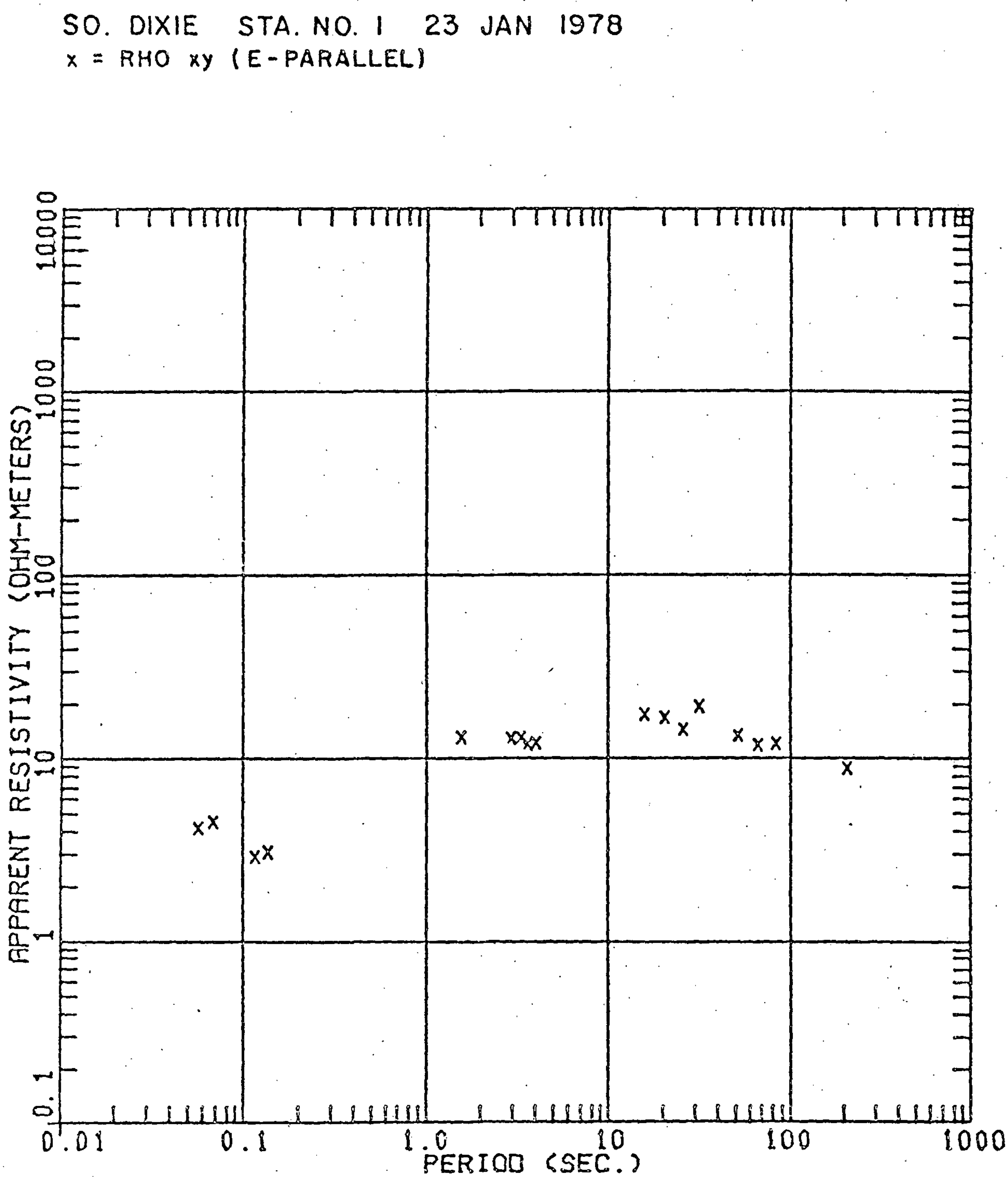

FIGURE 4. Apparent resistivity along the major axis of anisotropy at South Dixie Station #1 (average rotation angle = 56 degrees).

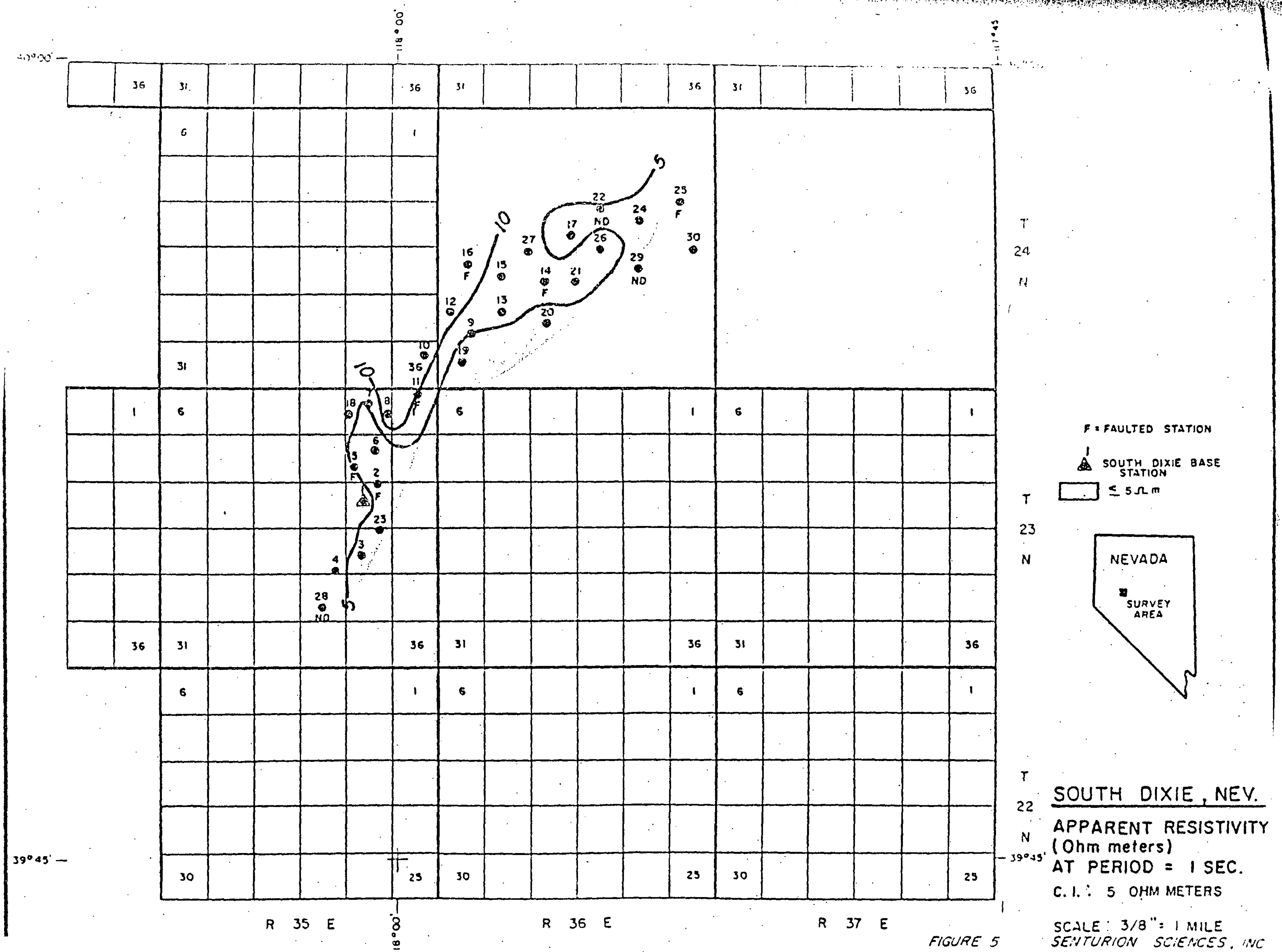

40°00'
118°00'
117°45'
39°45'
T 24 N
T 23 N
T 22 N
R 35 E
R 36 E
R 37 E
F = FAULTED STATION
SOUTH DIXIE BASE STATION
≤ 5 Ω m
NEVADA
SURVEY AREA
SOUTH DIXIE, NEV.
APPARENT RESISTIVITY (Ohm meters) AT PERIOD = 1 SEC.
C.I. : 5 OHM METERS
SCALE : 3/8" = 1 MILE
SENTURION SCIENCES, INC

FIGURE 5

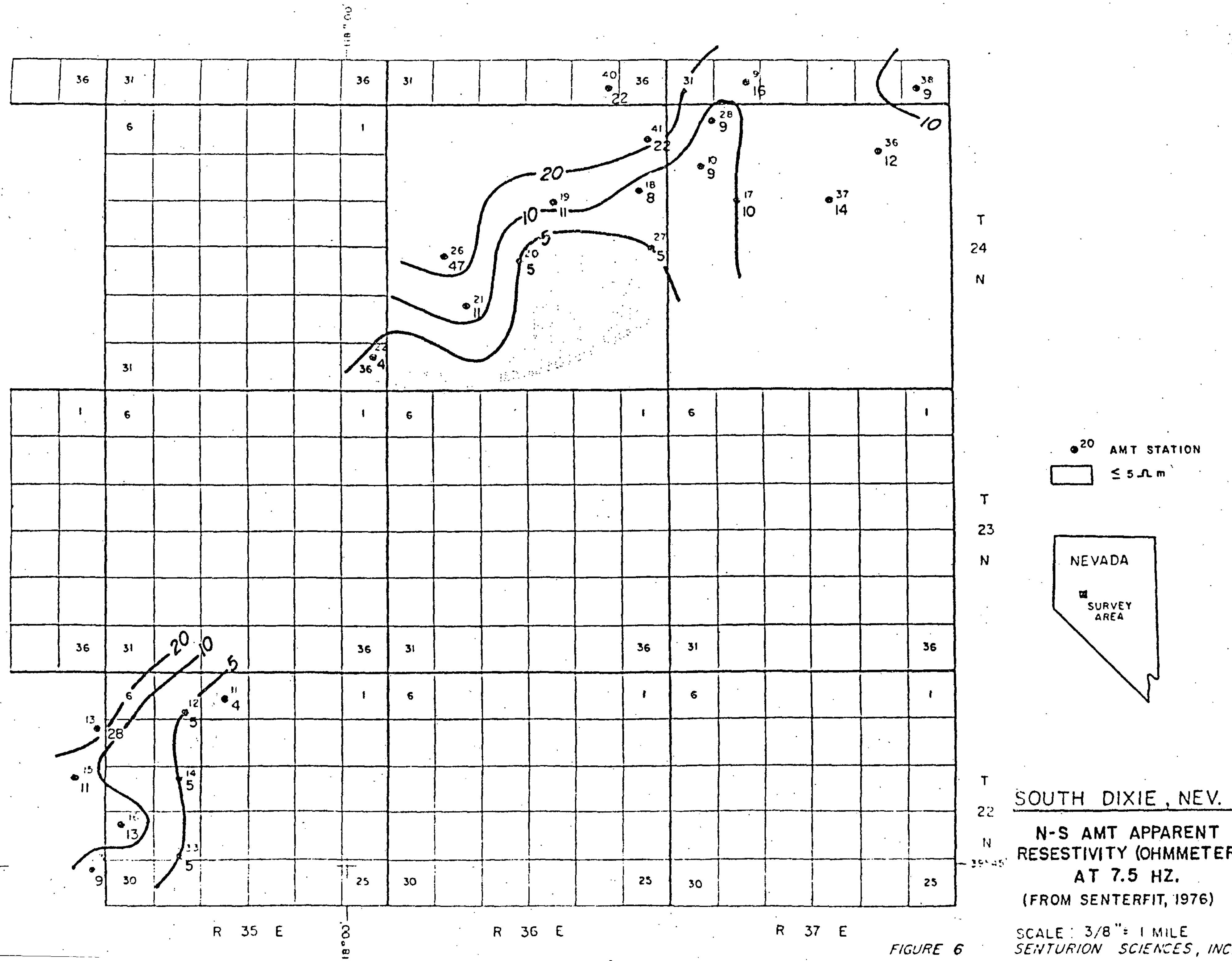

SOUTH DIXIE, NEV.

N-S AMT APPARENT RESESTIVITY (OHMMETER) AT 7.5 HZ.

(FROM SENTERFIT, 1976)

SCALE: 3/8" = 1 MILE

SENTURION SCIENCES, INC.

FIGURE 6

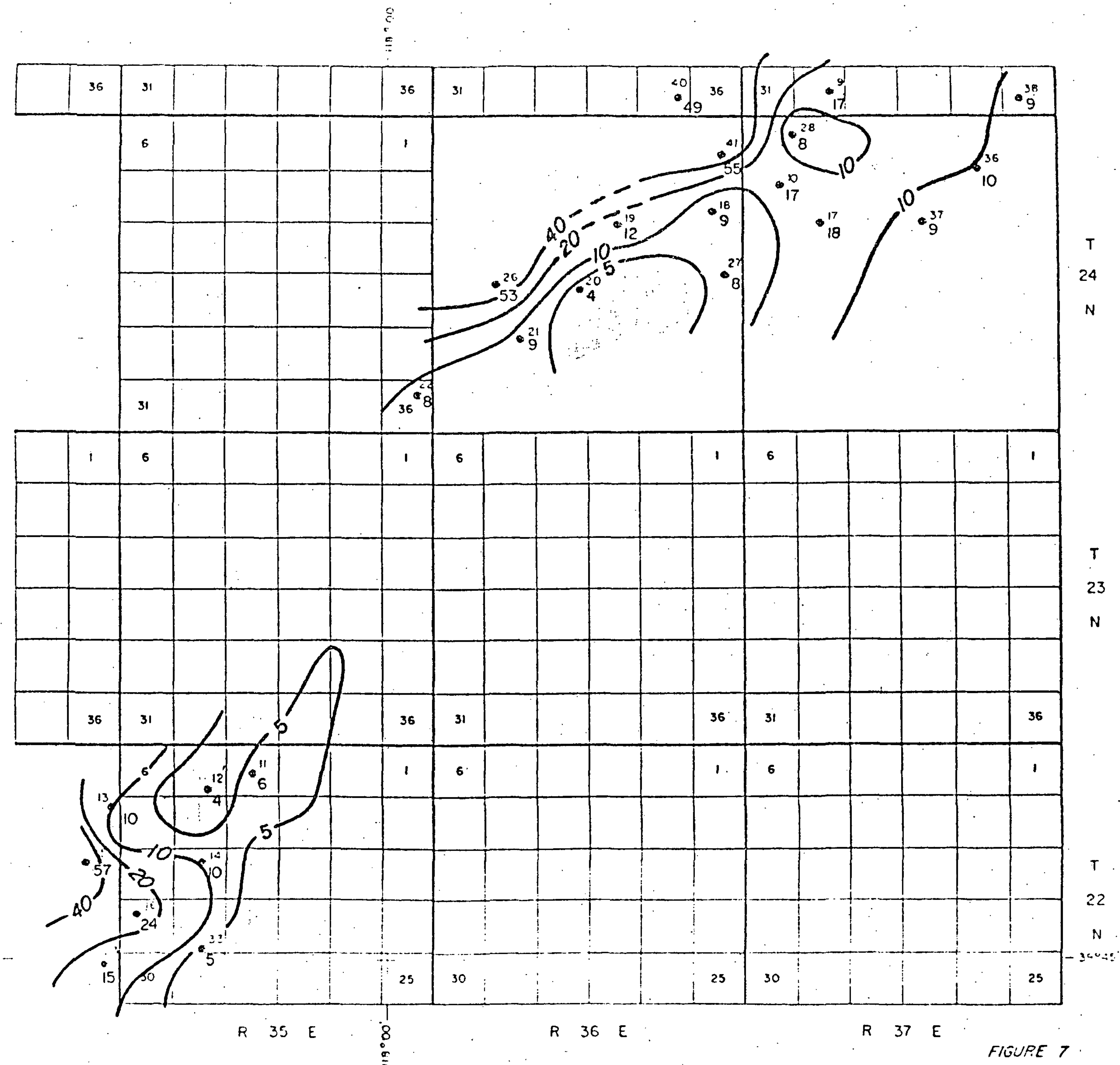

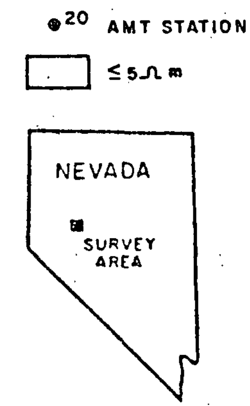

SOUTH DIXIE, NEV.

E-W AMT APPARENT RESISTIVITY (OHMMETER) AT 7.5 HZ.

FROM SENTERFIT, 1976

SCALE: 3/8" = 1 MILE

SENTURION SCIENCES, INC.

FIGURE 7

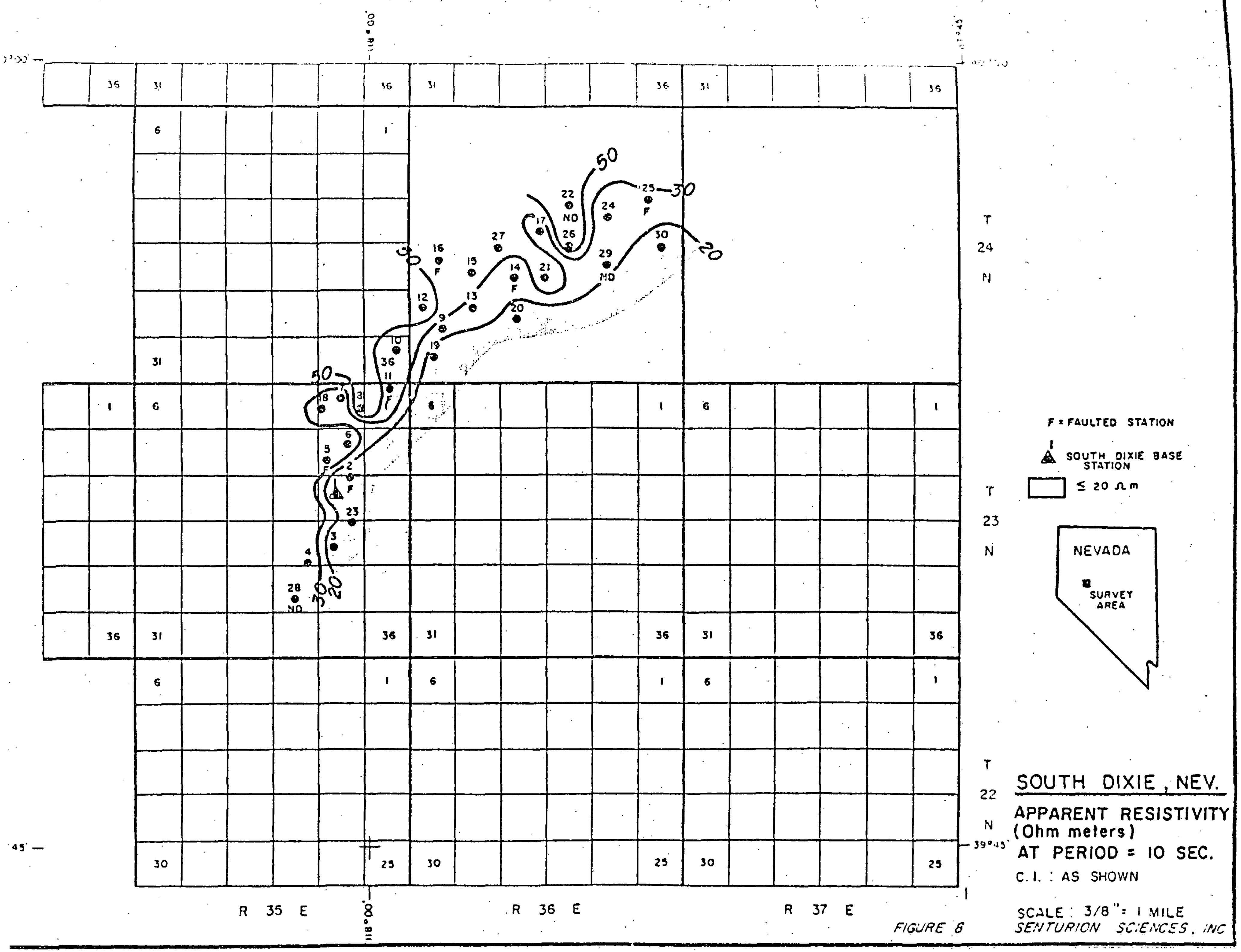

SOUTH DIXIE, NEV.
APPARENT RESISTIVITY (Ohm meters) AT PERIOD = 10 SEC.
C.I. : AS SHOWN
SCALE : 3/8" = 1 MILE
SENTURION SCIENCES, INC

FIGURE 8

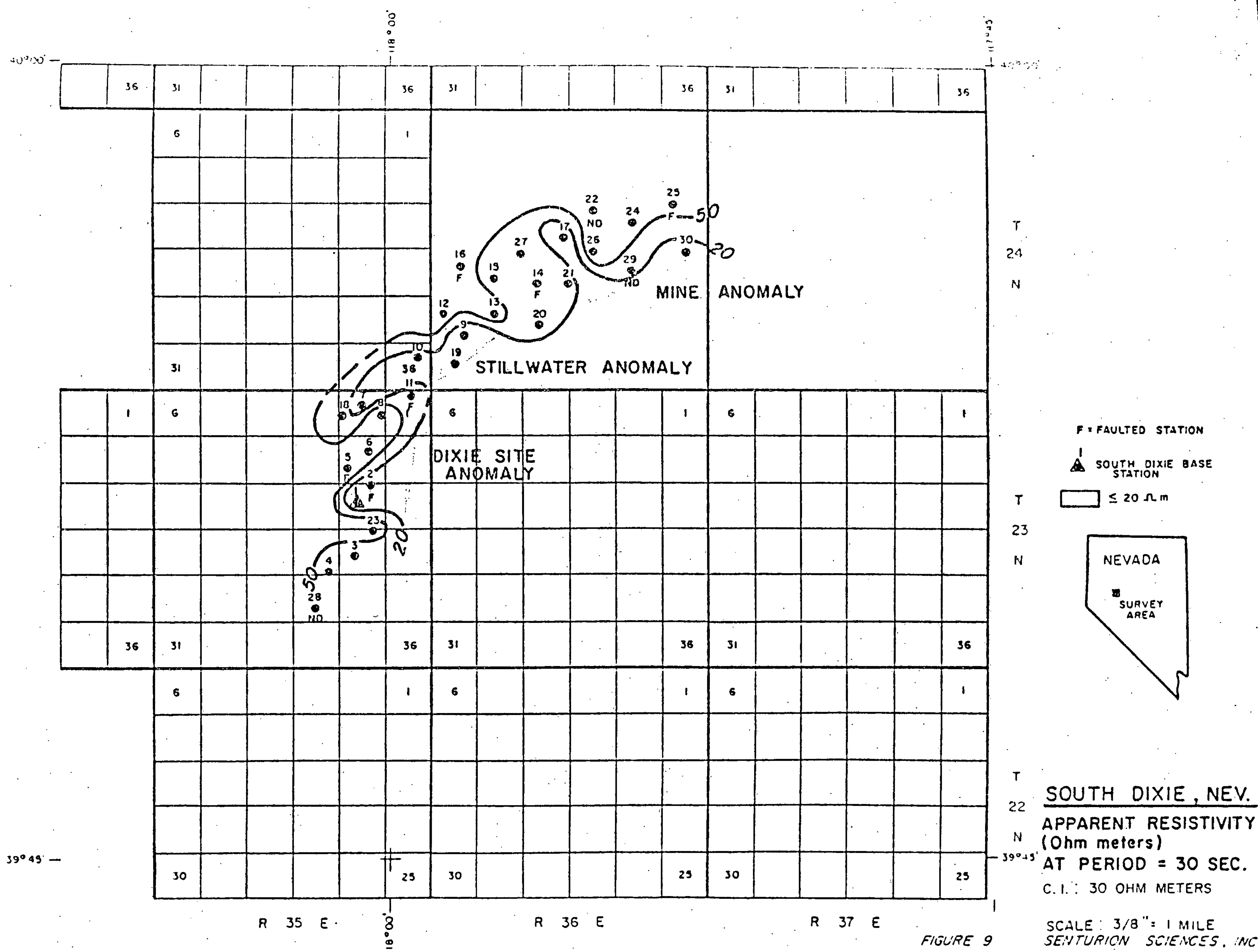

SOUTH DIXIE, NEV.
APPARENT RESISTIVITY (Ohm meters) AT PERIOD = 30 SEC.
C.I.: 30 OHM METERS
SCALE: 3/8" = 1 MILE
SENTURION SCIENCES, INC

FIGURE 9

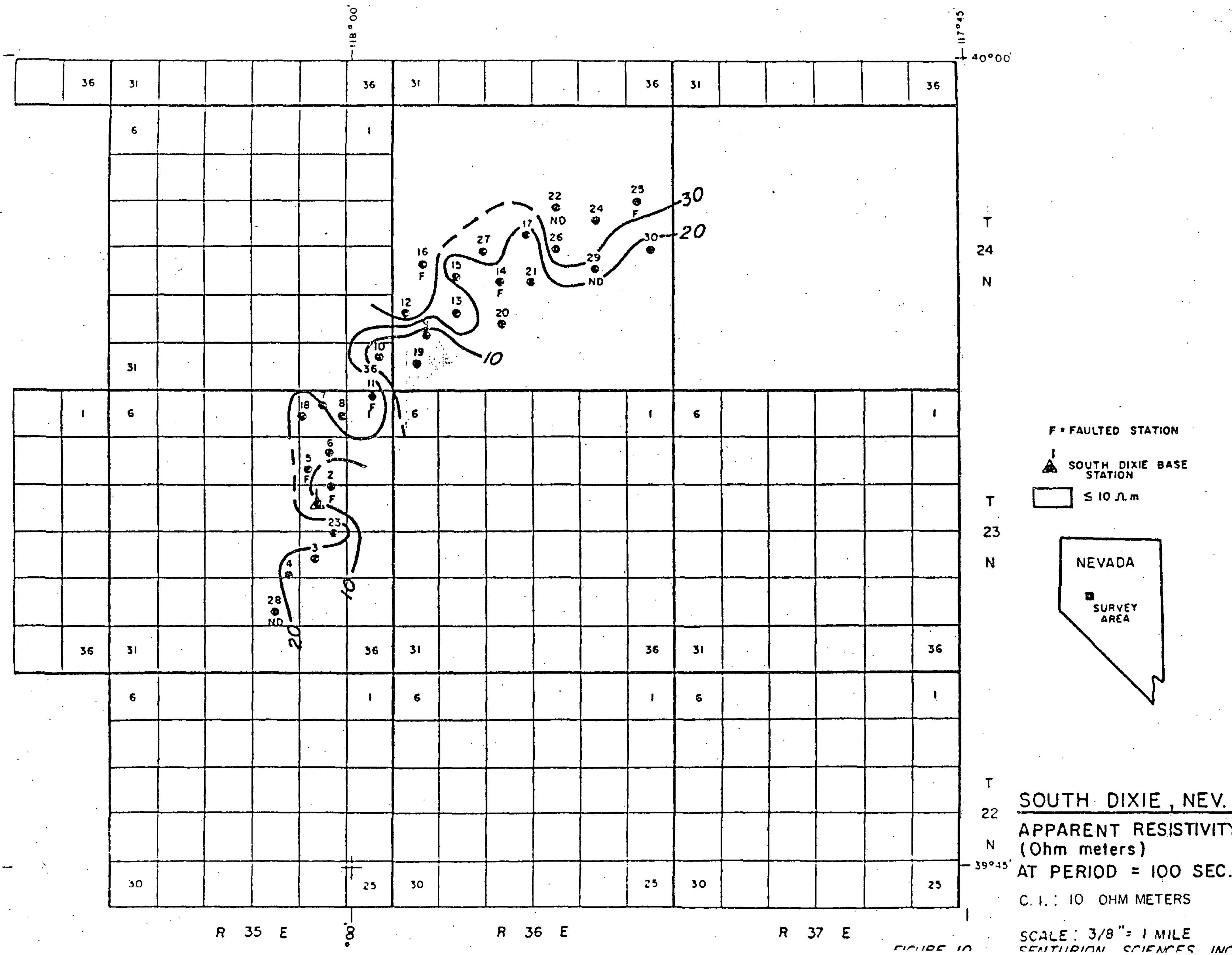

SOUTH DIXIE, NEV.

APPARENT RESISTIVITY (Ohm meters) AT PERIOD = 100 SEC.

C. I.: 10 OHM METERS

SCALE: 3/8" = 1 MILE

FIGURE 10

SENTURION SCIENCES, INC.

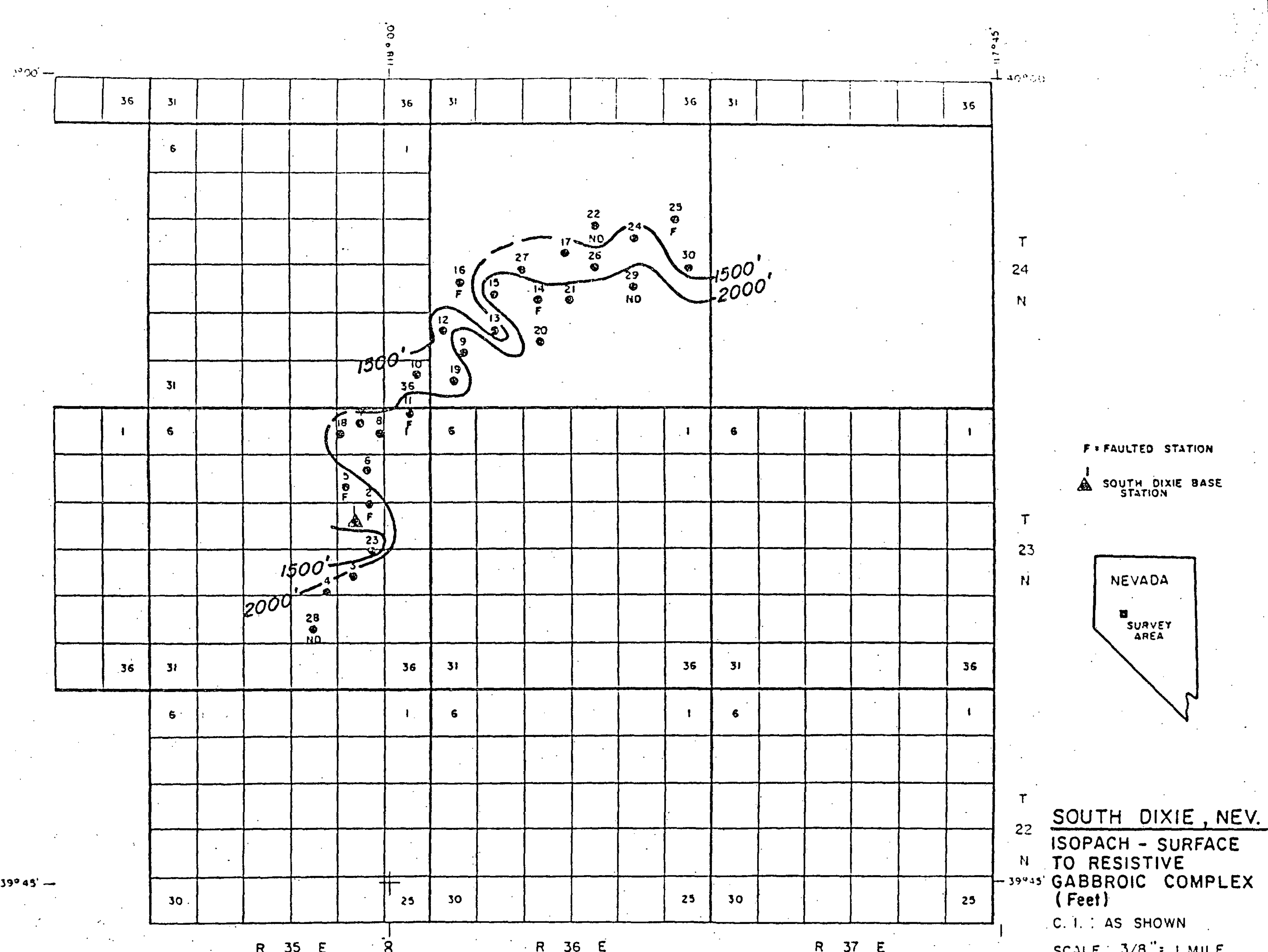

FIGURE 11

SENTURION SCIENCES, INC.

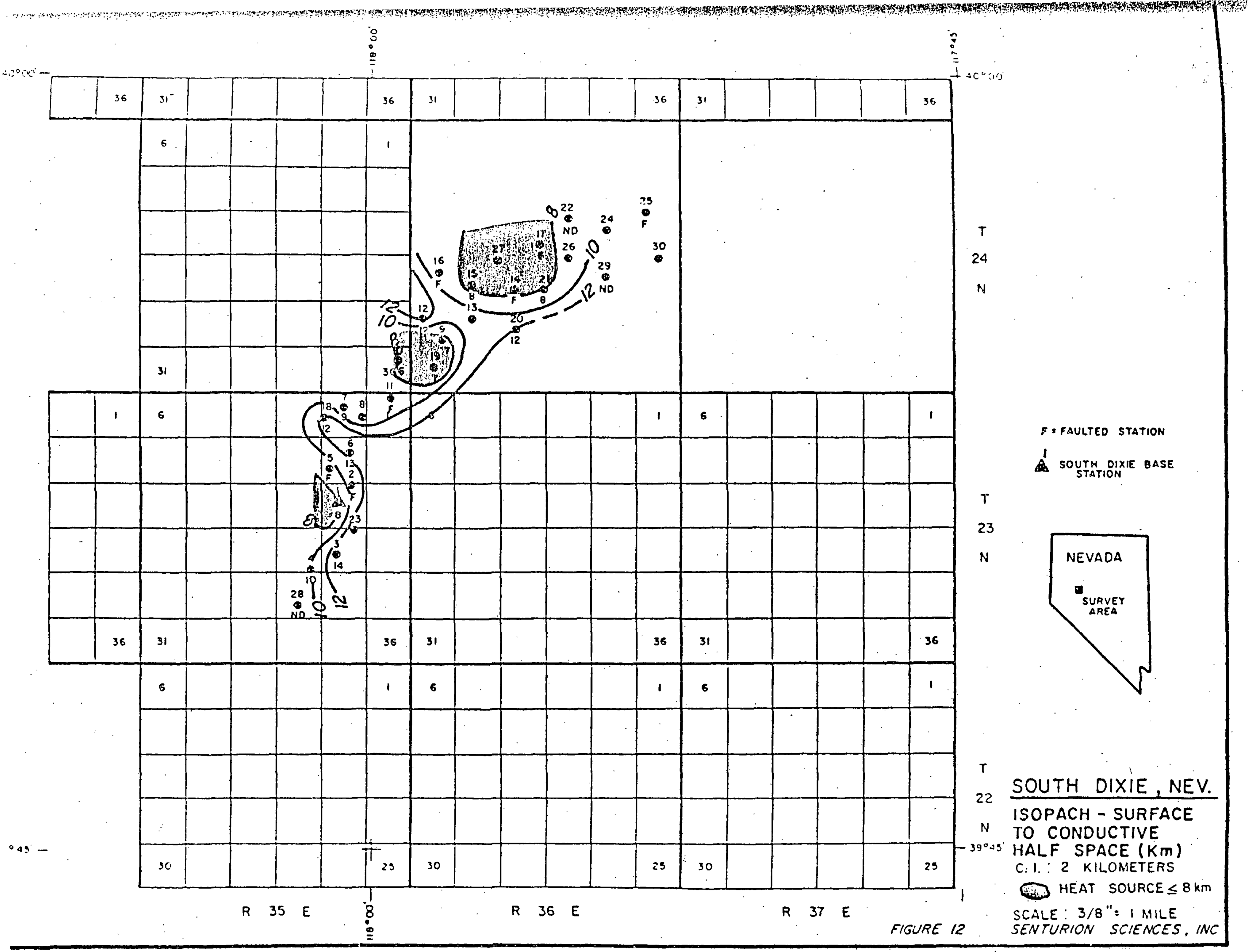

SOUTH DIXIE, NEV.
ISOPACH - SURFACE TO CONDUCTIVE HALF SPACE (Km)
C.I.: 2 KILOMETERS
HEAT SOURCE ≤ 8 km
SCALE: 3/8" = 1 MILE
SENTURION SCIENCES, INC
F = FAULTED STATION
SOUTH DIXIE BASE STATION
NEVADA
SURVEY AREA
T 24 N
T 23 N
T 22 N
R 35 E
R 36 E
R 37 E

FIGURE 12

REFERENCES

QUIGLEY, M. D., 1977; *High-Precision MultiLevel Aeromagnetic Survey of Dixie Valley, Nevada*, Southland Royalty task.

SENTERFIT, R. M., Donald Hoover and Charles Tippins, 1976; *Audio-magnetotelluric Data Log and Station Location Map for the Dixie Valley Known Geothermal Resource Area (KGRA), Nevada*, USGS Open File Report #76-292, Denver, Colorado.

SMITH, Thomas E., 1968; *Aeromagnetic Measurements in Dixie Valley, Nevada; Implications on Basin-Range Structure*, Journal of Geophysical Research, v. 73, no. 4, pp. 1321-1331.

STANLEY, W. D., J. E. Boehl, F. X. Bostick and H. W. Smith, 1977; *Geothermal Significance of Magnetotelluric Sounding in the Eastern Snake River Plain - Yellowstone Region*, Journal of Geophysical Research, v. 82, n. 17, pp. 2501-2514.

WILLDEN, Ronald, and Robert C. Speed, 1974; *Geology and Mineral Deposits of Churchill County, Nevada*, Bulletin 83, Nevada Bureau of Mines and Geology, University of Nevada, Reno.

APPENDIX

SURVEY PROCEDURES AND MT TECHNIQUE

The scalar magnetotelluric survey was run with a base station (station 1) which remained in one location for the duration of the survey. It continuously recorded one component of the telluric field and one component of the magnetic field perpendicular to the telluric field. The magnetometer was a Scintrex High Sensitivity Fluxgate Magnetometer. Field stations were identical to the base in configuration except that they did not record the magnetic field. A typical record low pass filtered at 0.1 Hz is shown in Figure A-1, a block diagram of the system in Figure A-2 and the system response curve in Figure A-3. Typical telluric amplifier gains were 2500 to 3000.

The 24 hours of data recorded at each station was played back, and a compressed oscillographic record made. A length (more than three hours and less than 10 hours) of data was spectrally analyzed using the compressed record as a guide to the best data interval. The telluric spectra at each station were normalized to the telluric spectra of the base station made over the same time interval. WWVB recorded continuously at each station made accurate time alignment possible. The normalized power spectra at the field stations were then multiplied by the sounding curve for the base stations to yield the apparent resistivity versus period graph for the field stations.

The magnetotelluric data for each station was inverted to a model of true resistivity with depth. This was done by computer, using a generalized linear inverse scheme similar to methods used to invert D.C. resistivity and vertical magnetic dipole data (Inman, *et al*, 1973, Glen, *et al*, 1973). This method of inversion assumes a horizontally layered earth without later variations in lithology and structure. These assumptions were clearly violated at many of the stations. This is evidenced primarily by the ascending branch (at long periods) of the sounding curves attaining a slope greater than 45° (the theoretical maximum for a layered earth). Trial and error modeling is the only method of quantitative interpretation that has been developed to handle these cases. In lieu of such a method of interpretation, we feel that a simple layered earth model at each station is the most reliable way of getting usable results.

Next to the sounding curve is the model (two to four layers) generated by the generalized linear inverse program. Superimposed on the data is the theoretical response of the model. The match between the observed data and the theoretical response varies in quality, but on the whole the match is good, especially in light of the complicated geology.

Apparent Resistivity. Apparent resistivities are calculated from the relative strengths of the magnetic and telluric fields at a station. These calculations performed at various frequencies (in our case, from 25 to 0.01 Hz) are made assuming that the earth is homogeneous or uniform in its electrical properties. Obviously, the earth is not homogeneous;

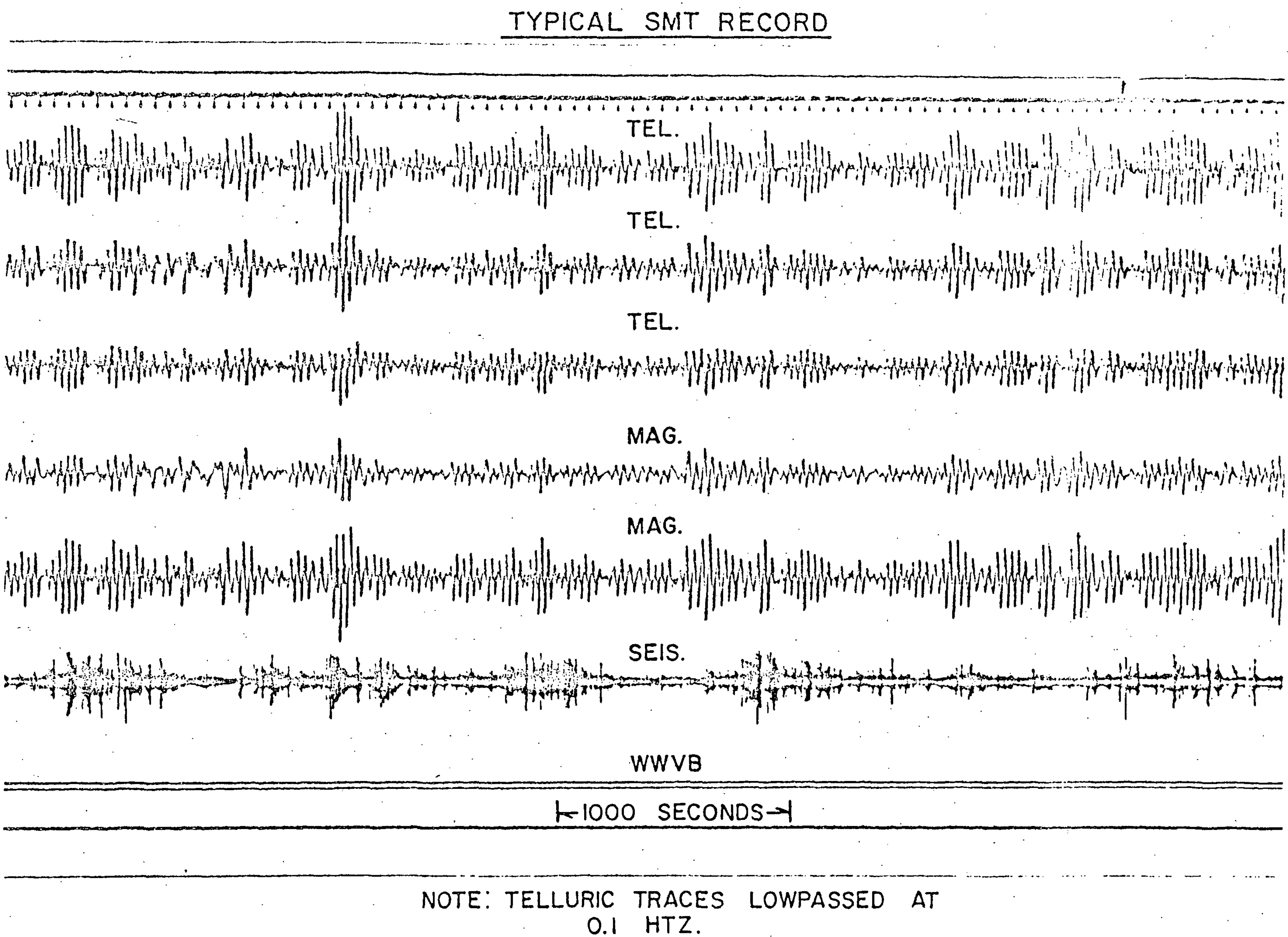
TYPICAL SMT RECORD
TEL.
TEL.
TEL.
MAG.
MAG.
SEIS.
WWVB
1000 SECONDS
NOTE: TELLURIC TRACES LOWPASSED AT
0.1 HTZ.

Figure A-1.

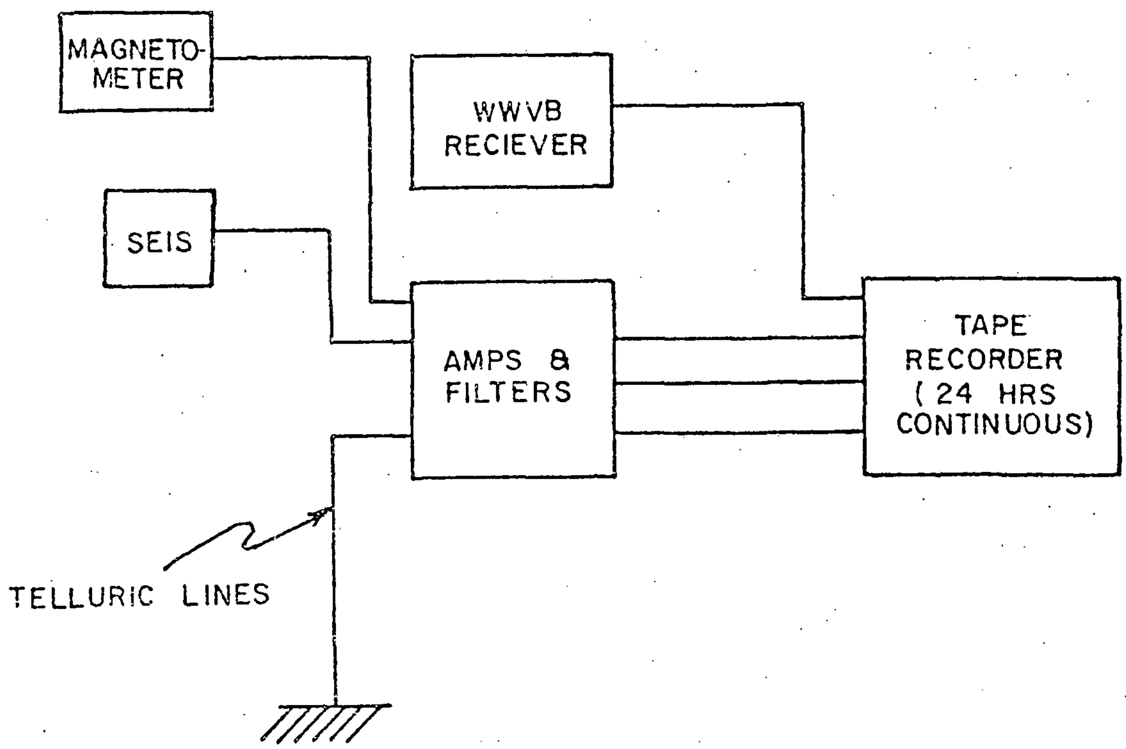

TELLURIC SYSTEM DIAGRAM

Figure A-2

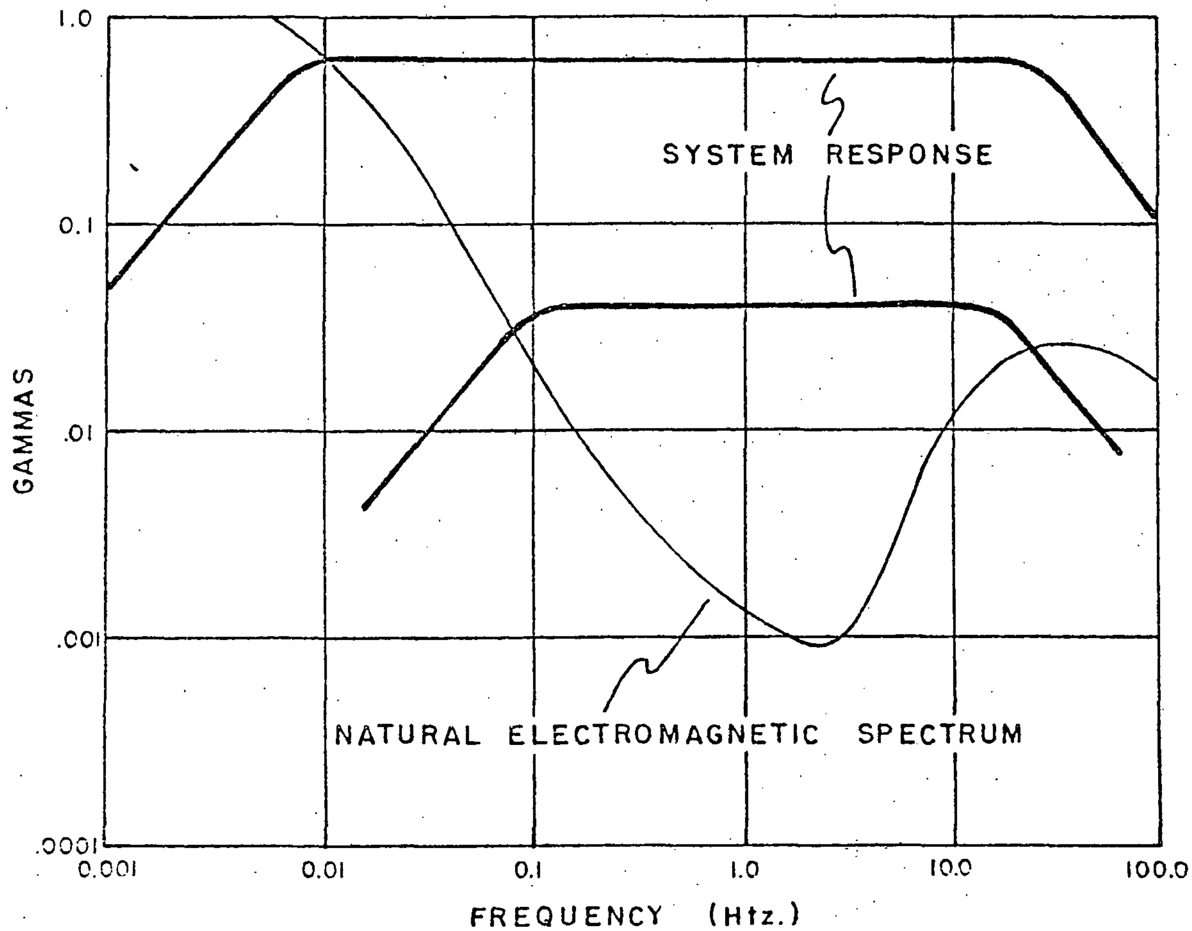

SYSTEM RESPONSE & TYPICAL NATURAL ELECTROMAGNETIC SPECTRUM so these calculated resistivities are apparent resistivities. A major part of the interpretation of magnetotellurics is the conversion of the apparent resistivity versus frequency to true resistivity versus depth.

Electrical Basement. The vast majority of magnetotelluric soundings made show increasing apparent resistivity at low frequencies. This is due to various causes, the principal one being the fact that at most places in the earth, low resistivity material lies over high resistivity material. This is the case, for example, in an alluvial-filled valley in the Basin and Range or sedimentary section over Precambrian basement in the Mid-Continent. This large jump in resistivity at depth is called the electrical basement. Obviously, it is not the same horizon everywhere; in fact, the structure which forms electrical basement at any given place may be high in the section compared to what a geologist would call basement rock. The configuration of this electrical basement is often the most accurate information that MT can yield.

Another aspect of electrical basement is the fact that it often is difficult to determine electrical properties beneath this horizon. The particular horizon which acts as electrical basement may be thick limestone halfway down a sedimentary section with a resistivity contrast of 10 to 15, and although information nearly always can be had by extending the sounding to lower frequencies, considerable resolution is lost.

Inversion. The raw data used by an MT analyst is the sounding curve, which is a graph of apparent resistivity versus period of the electromagnetic field. To create a model of the subsurface whose response is the same as the observed data is called inversion. Formerly, this inversion was done by comparing the observed data with theoretical sounding curves for various earth models. Because any catalog of theoretical curves must be limited in size, many (in fact, most) observed sounding curves could not be found in the catalog. Although various mathematical devices were developed to combine and interpolate between theoretical curves, it was very difficult to get an adequate match with the observed data. Today, there are several mathematical algorithms that can be implemented on a computer that can perform an inversion better than the trial and error of curve matching. Senturion has developed a "generalized linear inverse" scheme to interpret our scalar MT data and give satisfactory models of true resistivity with depth.

Scalar and Tensor MT. The first systematic exposition of magnetotellurics was set forth by Louis Cagnaird in the early 1950's. His theory was that variations in the magnetic field in a given direction would induce telluric currents at right angles to this direction. By measuring the changes in the telluric field at right angles to this, one could measure the earth's electromagnetic impedance and derive resistivity information from this. Information at various depths came from the fact that the depth penetration of electromagnetic waves into the earth is inversely proportional to the frequency of the wave. According to Cagnaird's original theory, it should not matter which direction the magnetometer and telluric lines were set up; one would get the same result. When careful MT surveys were done, it was soon found that when one was near an abrupt lateral change such as a fault, the magentic field induced currents to flow in not just at right angles to the direction of polarization, but at every orientation (in differing amounts, depending on the geometry of the nearby structure). The mathematical theory developed to handle situations other than the simple layered earth has been named tensor magnetotellurics. The tensor theory explicitly takes into account the directional characteristics (or anisotropy) of the earth and structures within it and gives a mathematical foundation for interpreting the data in more complicated situations than the scalar MT of Cagnaird. In tensor MT, three components of the magentic field are recorded. This requires more data acquisition equipment and much more data processing and interpretation cost. Because of the cost of tensor MT equipment, it has not been feasible to do more than one tensor station at a time. Scalar MT, on the other hand, is relatively easy to accomplish and process, but it cannot give quantitative results in some geologic situations.

REFERENCES

GLEN, W. E., J. Ryn, S. H. Ward, W. J. Peeples and R. J. Phillips, 1973; *The Inversion of Vertical Magnetic Dipole Sounding Data*; Geophysics, v. 38, no. 6, pp. 1109-1129.

INMAN, Joseph R., R. Ryn and S. H. Ward, 1973; *Resistivity Inversion;* Geophysics, v. 38, no. 6, pp. 1088-1108

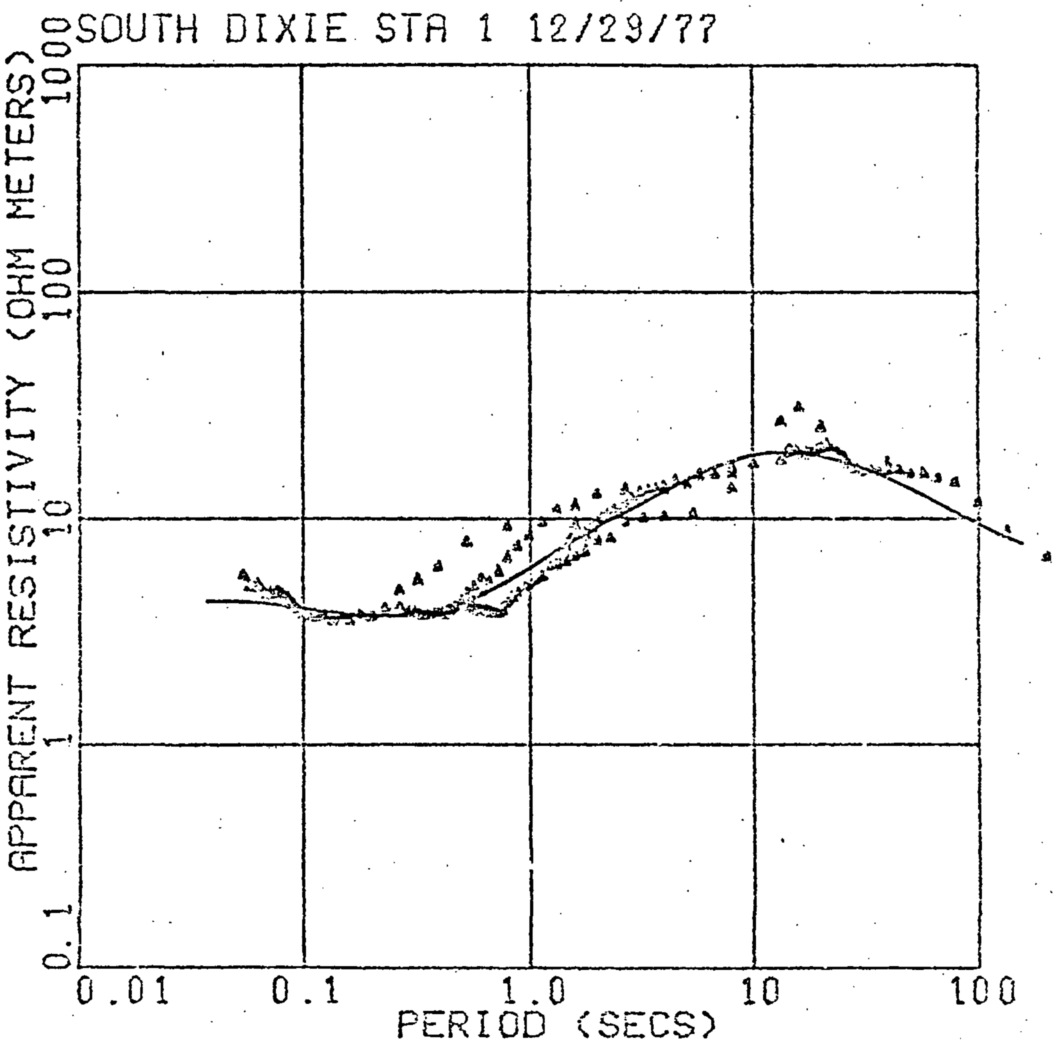
SOUTH DIXIE STA 1 12/29/77
APPARENT RESISTIVITY (OHM METERS)
1000
100
10
1
0.1
0.01
0.1
1.0
10
100
PERIOD (SECS)

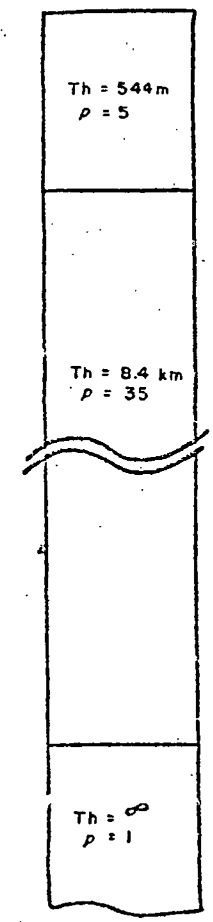
Th = 544m
ρ = 5
Th = 8.4 km
ρ = 35
Th = ∞
ρ = 1

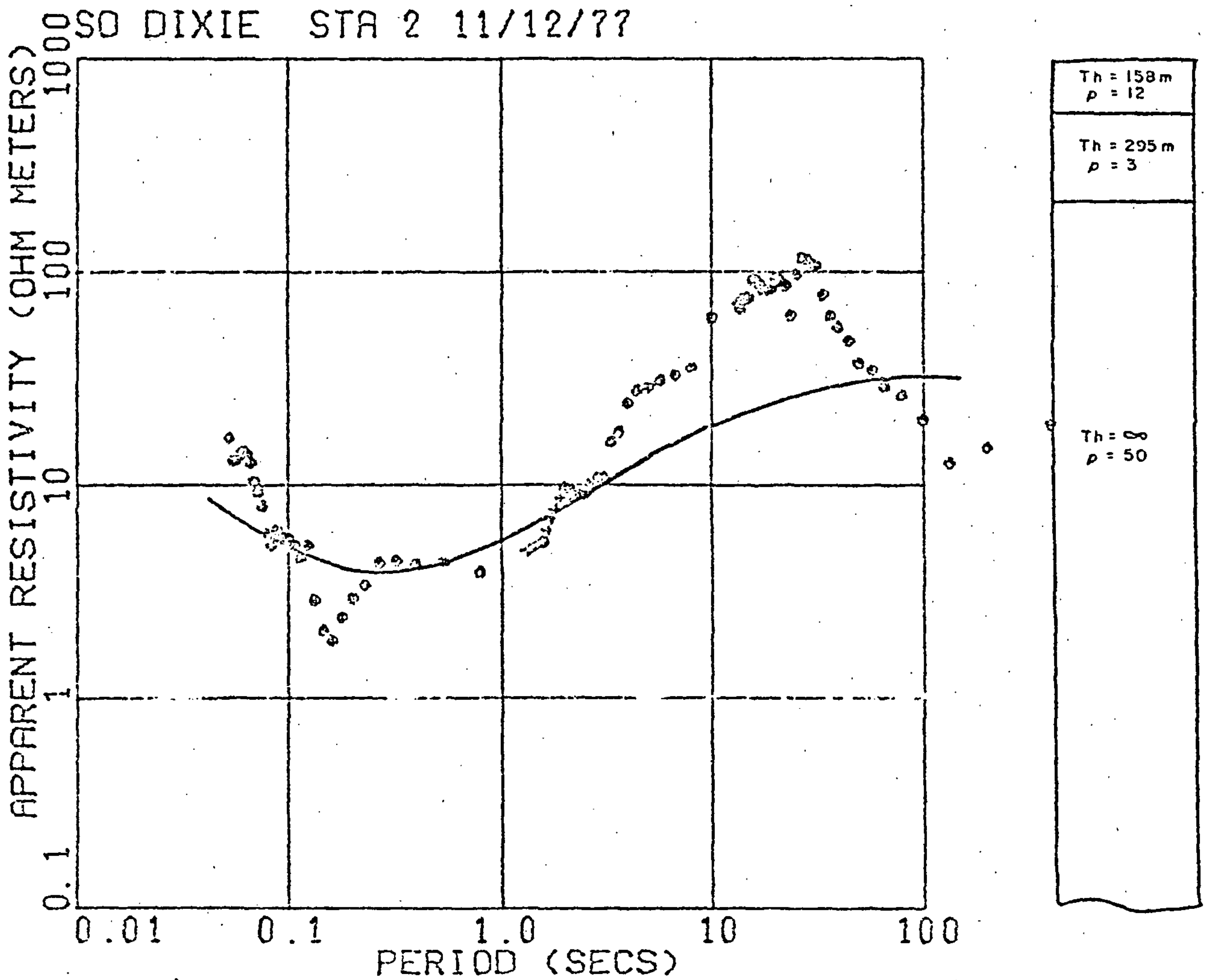
SO DIXIE STA 2 11/12/77
APPARENT RESISTIVITY (OHM METERS)
1000
100
10
1
0.1
0.01
0.1
1.0
10
100
PERIOD (SECS)
Th = 158 m
ρ = 12
Th = 295 m
ρ = 3
Th = ∞
ρ = 50

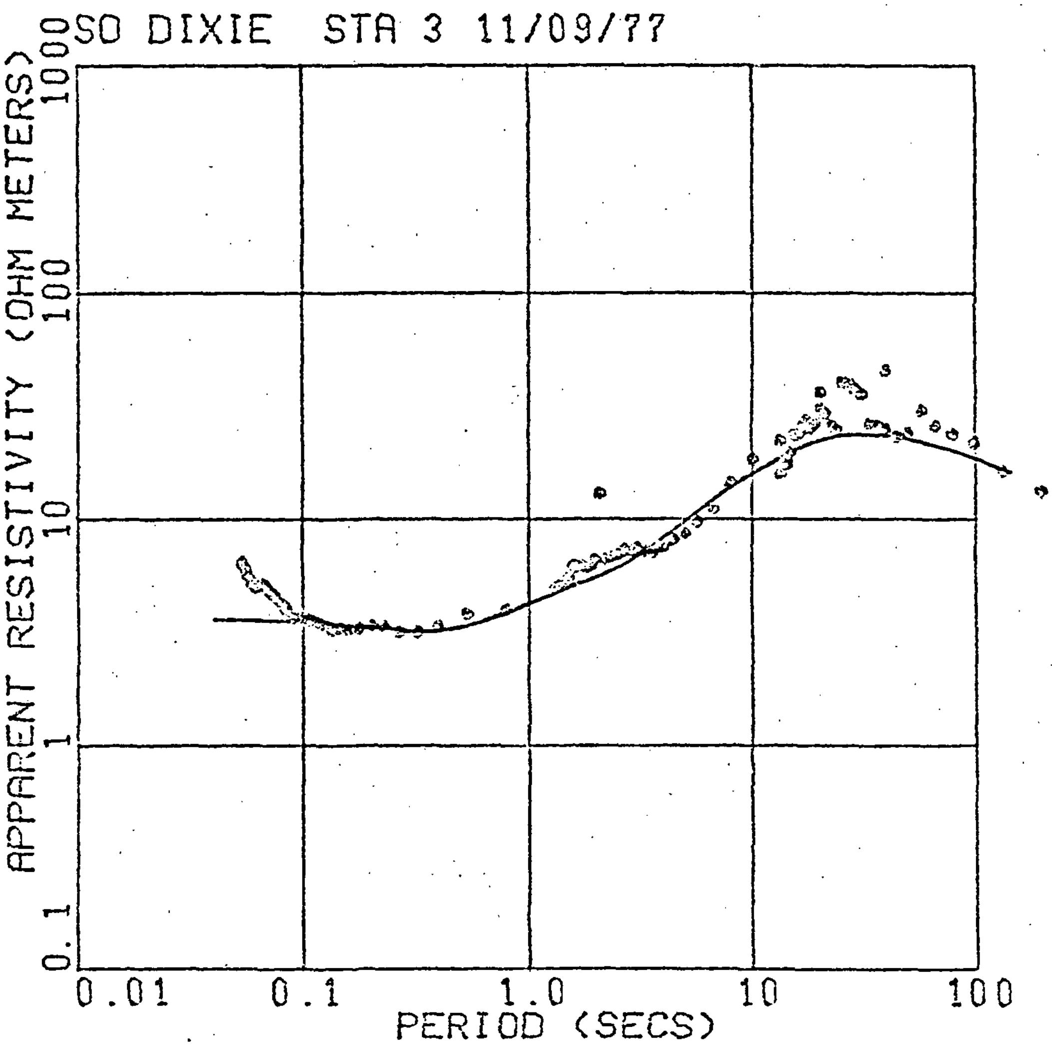

SO DIXIE STA 3 11/09/77
APPARENT RESISTIVITY (OHM METERS)
1000
100
10
1
0.1
0.01
0.1
1.0
10
100
PERIOD (SECS)

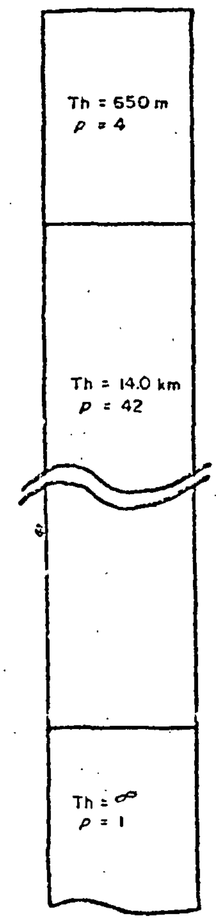

Th = 650 m
ρ = 4
Th = 14.0 km
ρ = 42
Th = ∞
ρ = 1

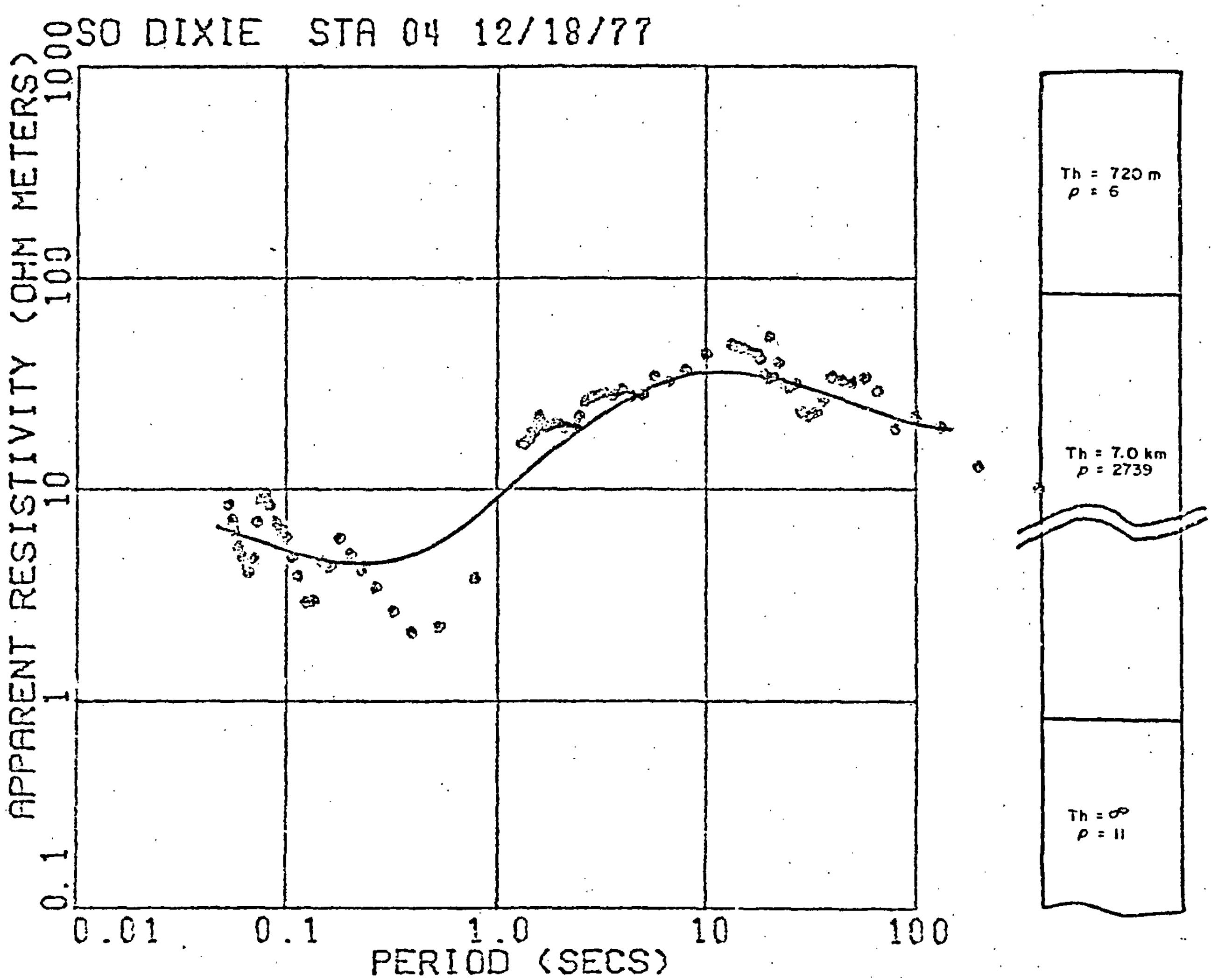
SO DIXIE STA 04 12/18/77
APPARENT RESISTIVITY (OHM METERS)
1000
100
10
1
0.1
0.01
0.1
1.0
10
100
PERIOD (SECS)
Th = 720 m
ρ = 6
Th = 7.0 km
ρ = 2739
Th = ∞
ρ = 11

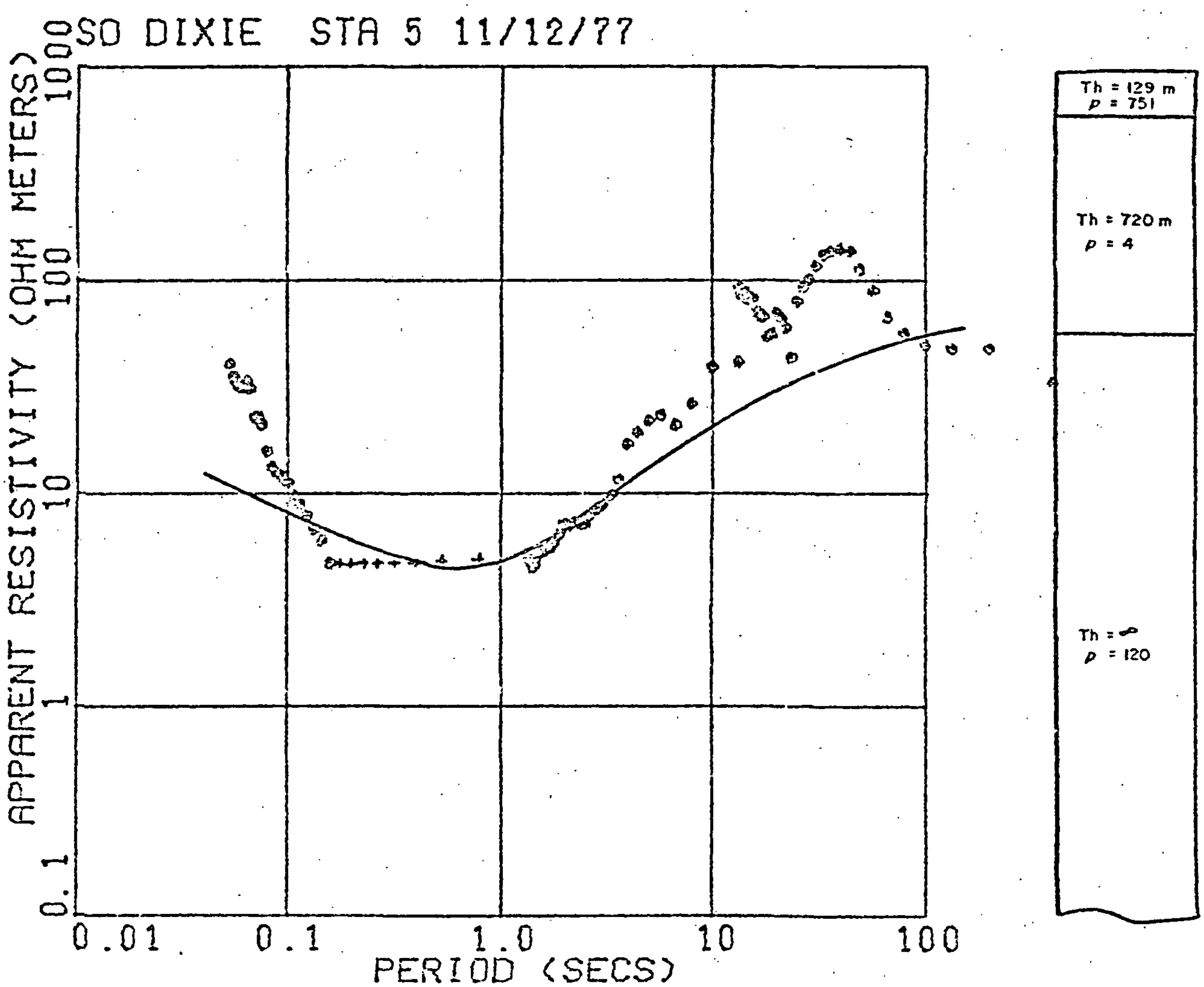
SO DIXIE STA 5 11/12/77
APPARENT RESISTIVITY (OHM METERS)
1000
100
10
1
0.1
0.01
0.1
1.0
10
100
PERIOD (SECS)
Th = 129 m
ρ = 751
Th = 720 m
ρ = 4
Th = ∞
ρ = 120

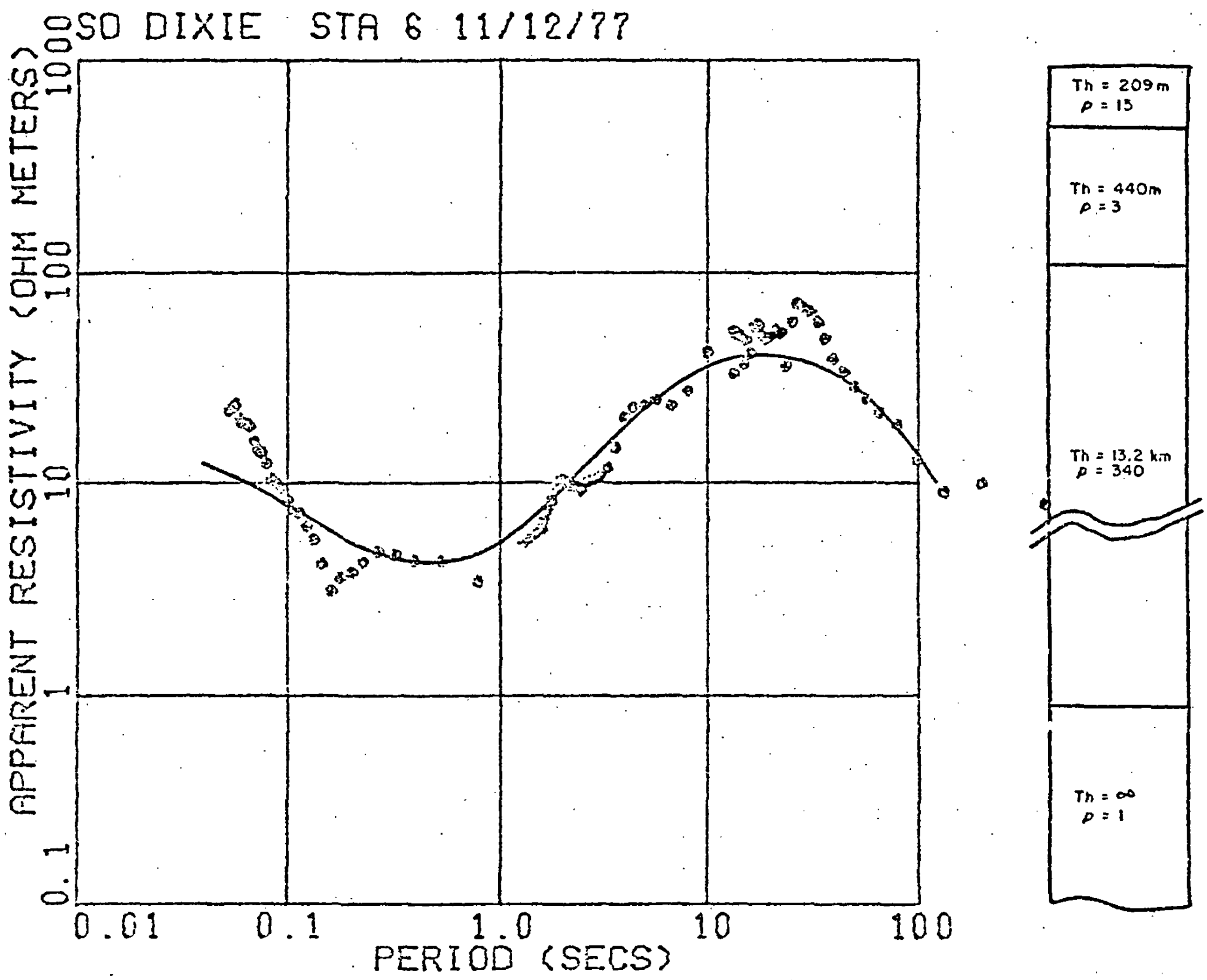
SO DIXIE STA 6 11/12/77
APPARENT RESISTIVITY (OHM METERS)
1000
100
10
1
0.1
0.01
0.1
1.0
10
100
PERIOD (SECS)
Th = 209m
ρ = 15
Th = 440m
ρ = 3
Th = 13.2 km
ρ = 340
Th = ∞
ρ = 1

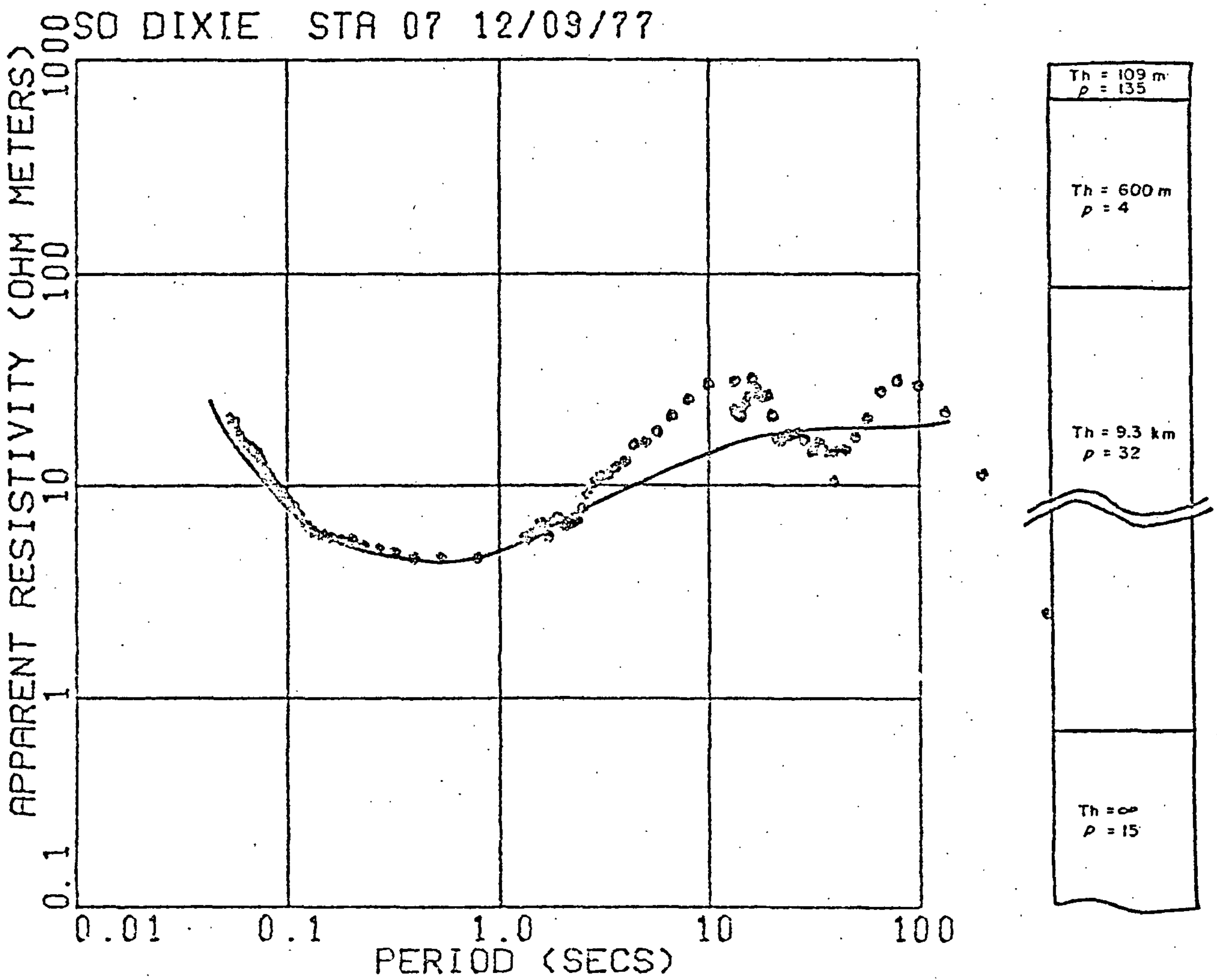
SO DIXIE STA 07 12/09/77
APPARENT RESISTIVITY (OHM METERS)
1000
100
10
1
0.1
0.01
0.1
1.0
10
100
PERIOD (SECS)
Th = 109 m
ρ = 135
Th = 600 m
ρ = 4
Th = 9.3 km
ρ = 32
Th = ∞
ρ = 15

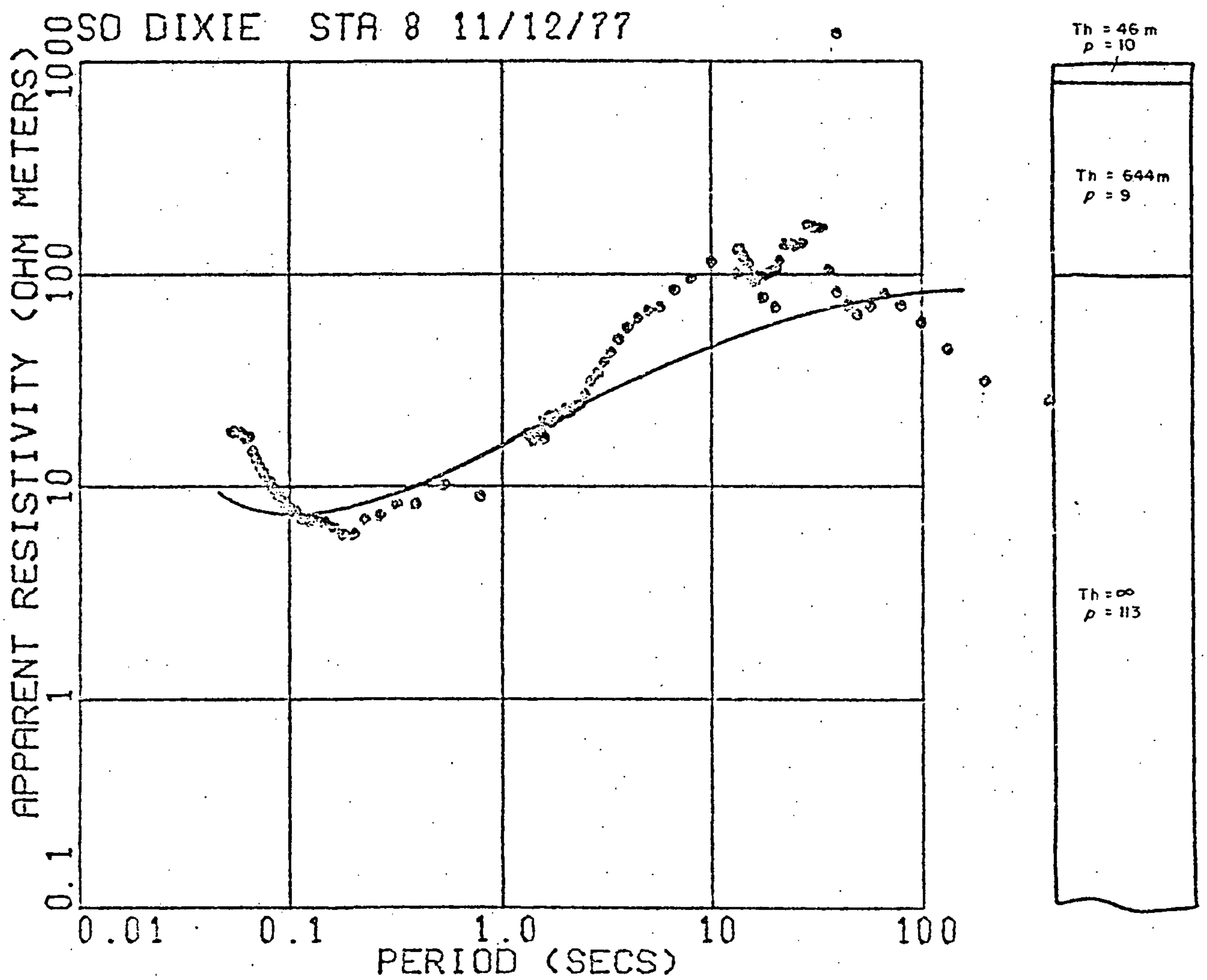

SO DIXIE STA 8 11/12/77
APPARENT RESISTIVITY (OHM METERS)
1000
100
10
1
0.1
0.01
0.1
1.0
10
100
PERIOD (SECS)
Th = 46 m
ρ = 10
Th = 644m
ρ = 9
Th = ∞
ρ = 113

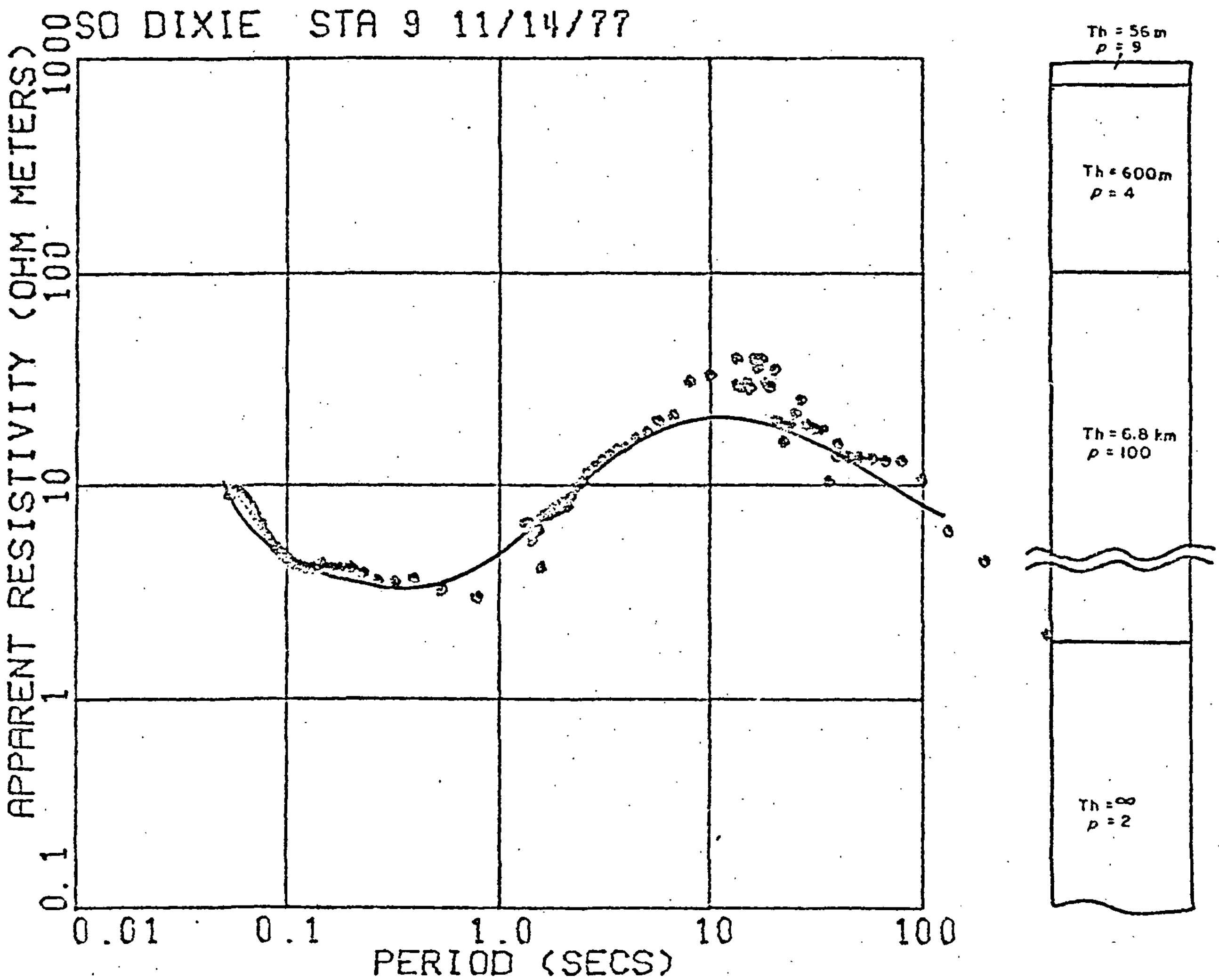
SO DIXIE STA 9 11/14/77
APPARENT RESISTIVITY (OHM METERS)
1000
100
10
1
0.1
0.01
0.1
1.0
10
100
PERIOD (SECS)
Th = 56 m
ρ = 9
Th = 600m
ρ = 4
Th = 6.8 km
ρ = 100
Th = ∞
ρ = 2

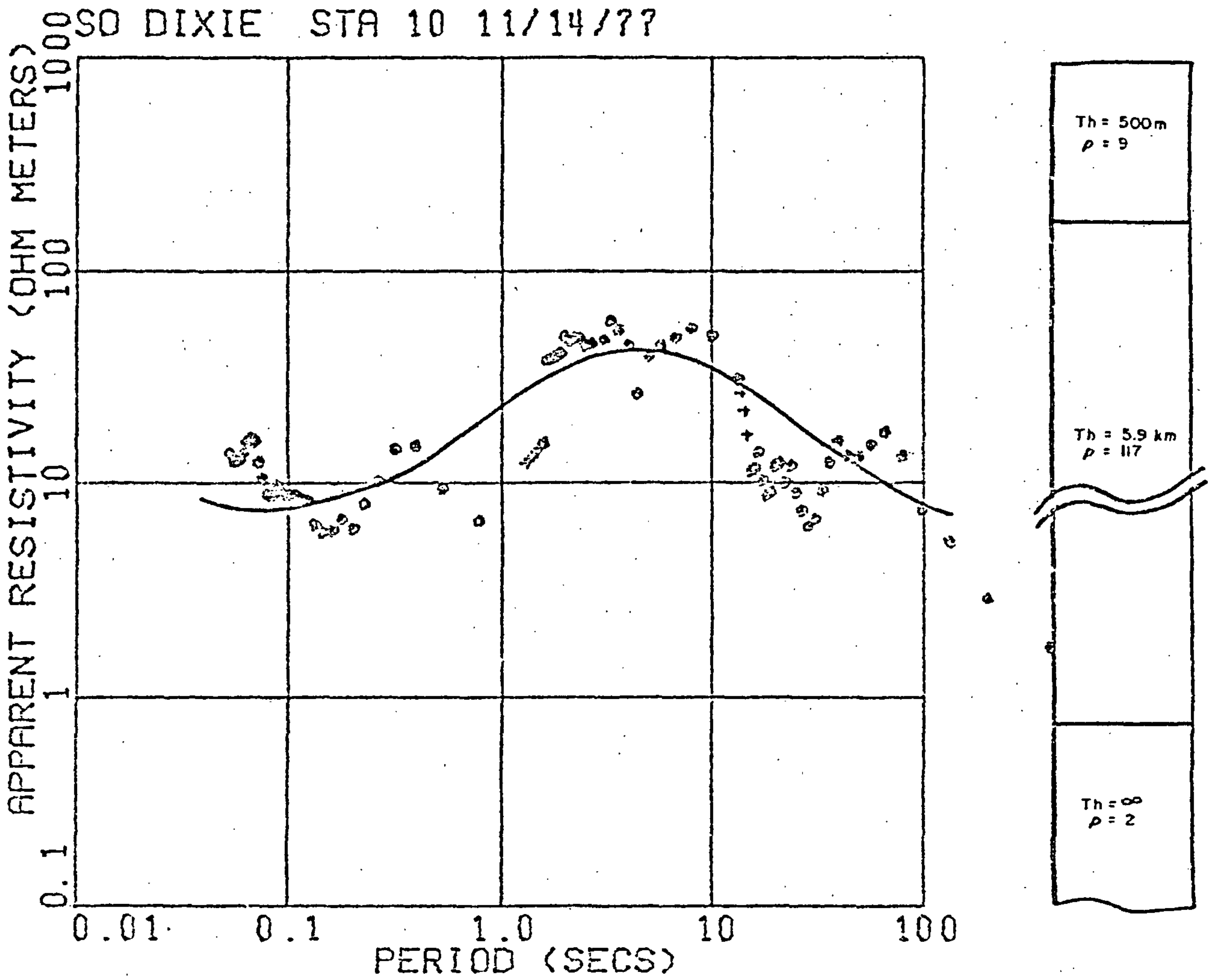
SO DIXIE STA 10 11/14/77
APPARENT RESISTIVITY (OHM METERS)
1000
100
10
1
0.1
0.01
0.1
1.0
10
100
PERIOD (SECS)
Th = 500m
ρ = 9
Th = 5.9 km
ρ = 117
Th = ∞
ρ = 2

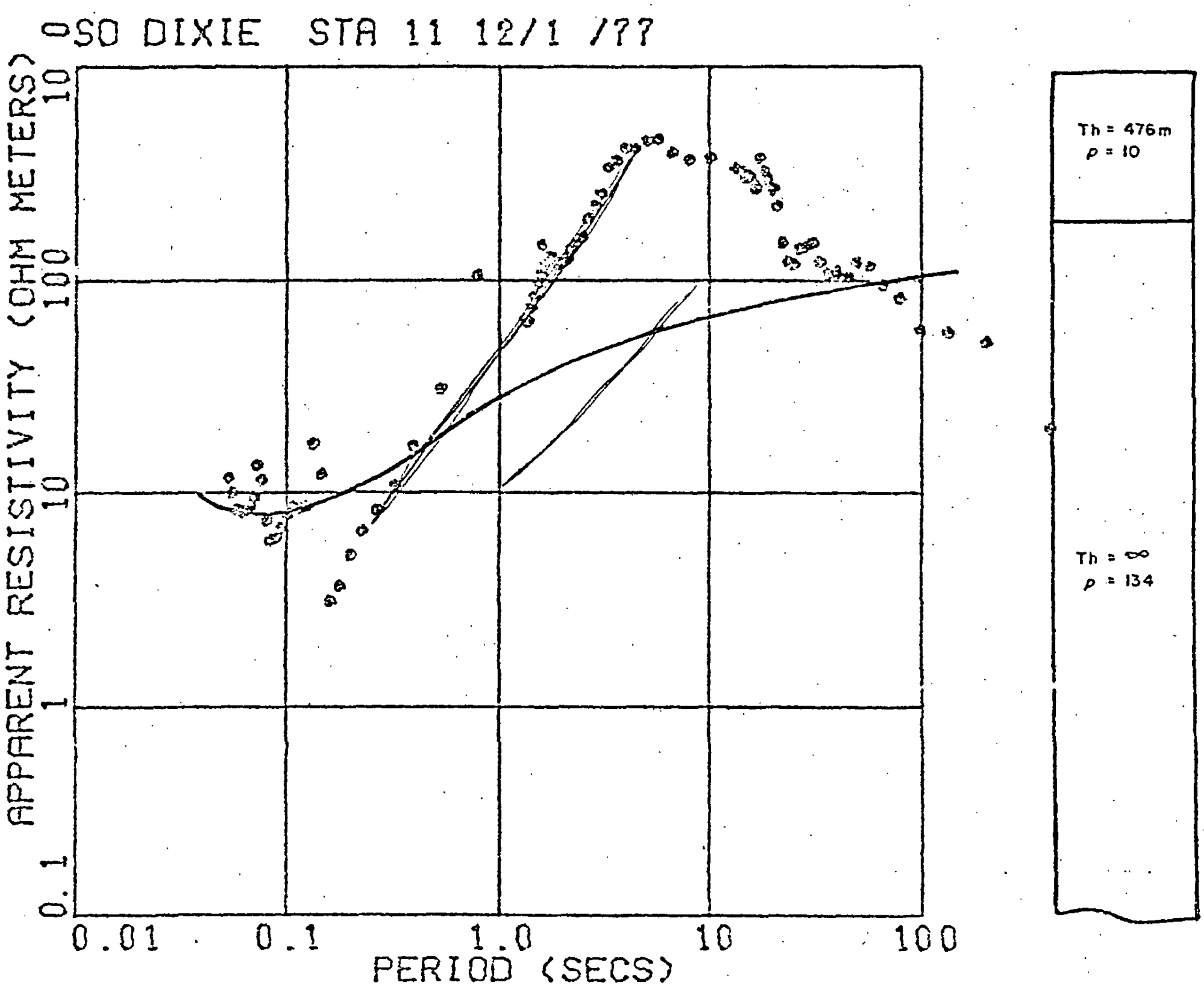

SO DIXIE STA 11 12/1 /77
APPARENT RESISTIVITY (OHM METERS)
0.1
1
10
100
0.01
0.1
1.0
10
100
PERIOD (SECS)
Th = 476m
ρ = 10
Th = ∞
ρ = 134

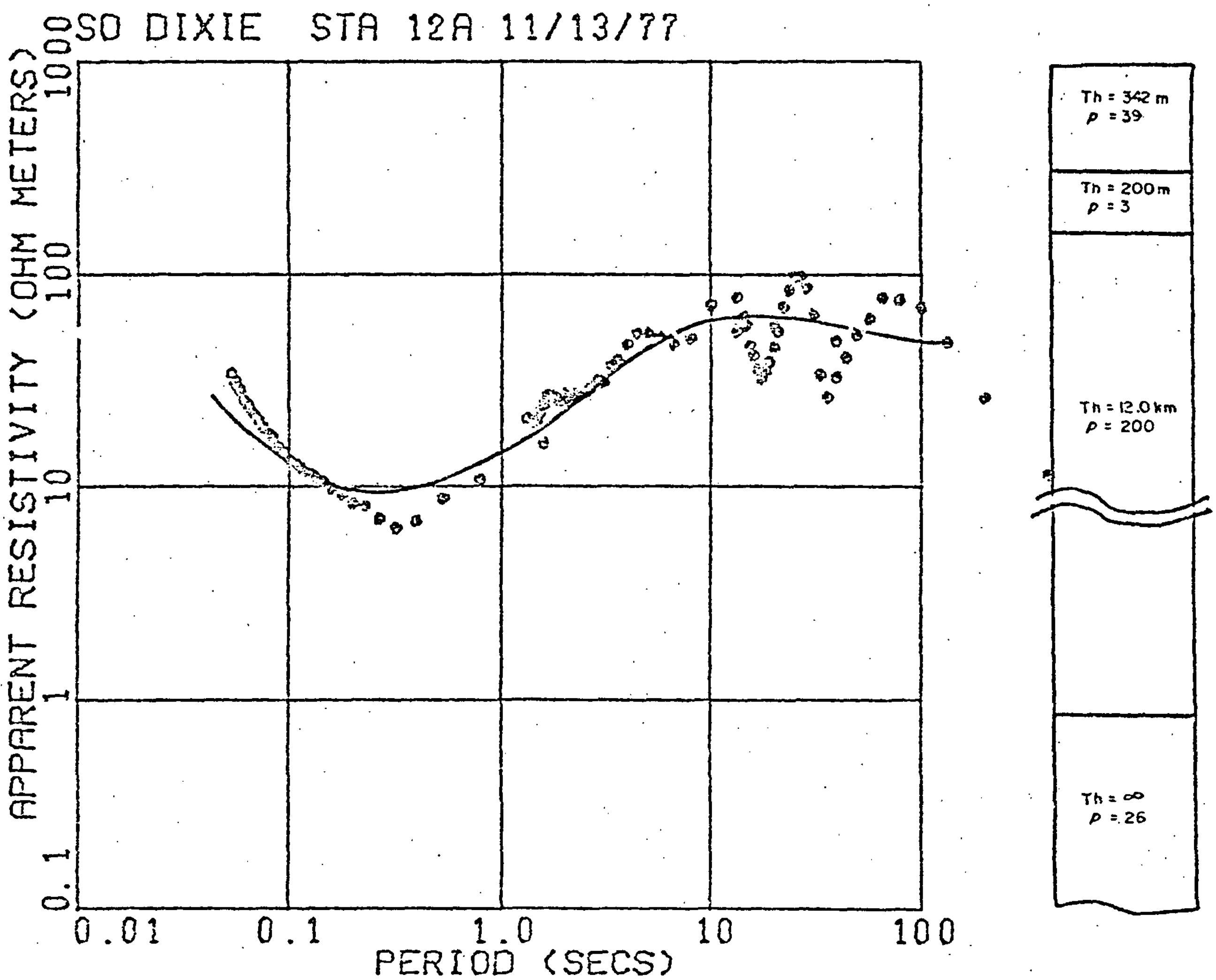
SO DIXIE STA 12A 11/13/77
APPARENT RESISTIVITY (OHM METERS)
1000
100
10
1
0.1
0.01
0.1
1.0
10
100
PERIOD (SECS)
Th = 342 m
ρ = 39
Th = 200 m
ρ = 3
Th = 12.0 km
ρ = 200
Th = ∞
ρ = 26

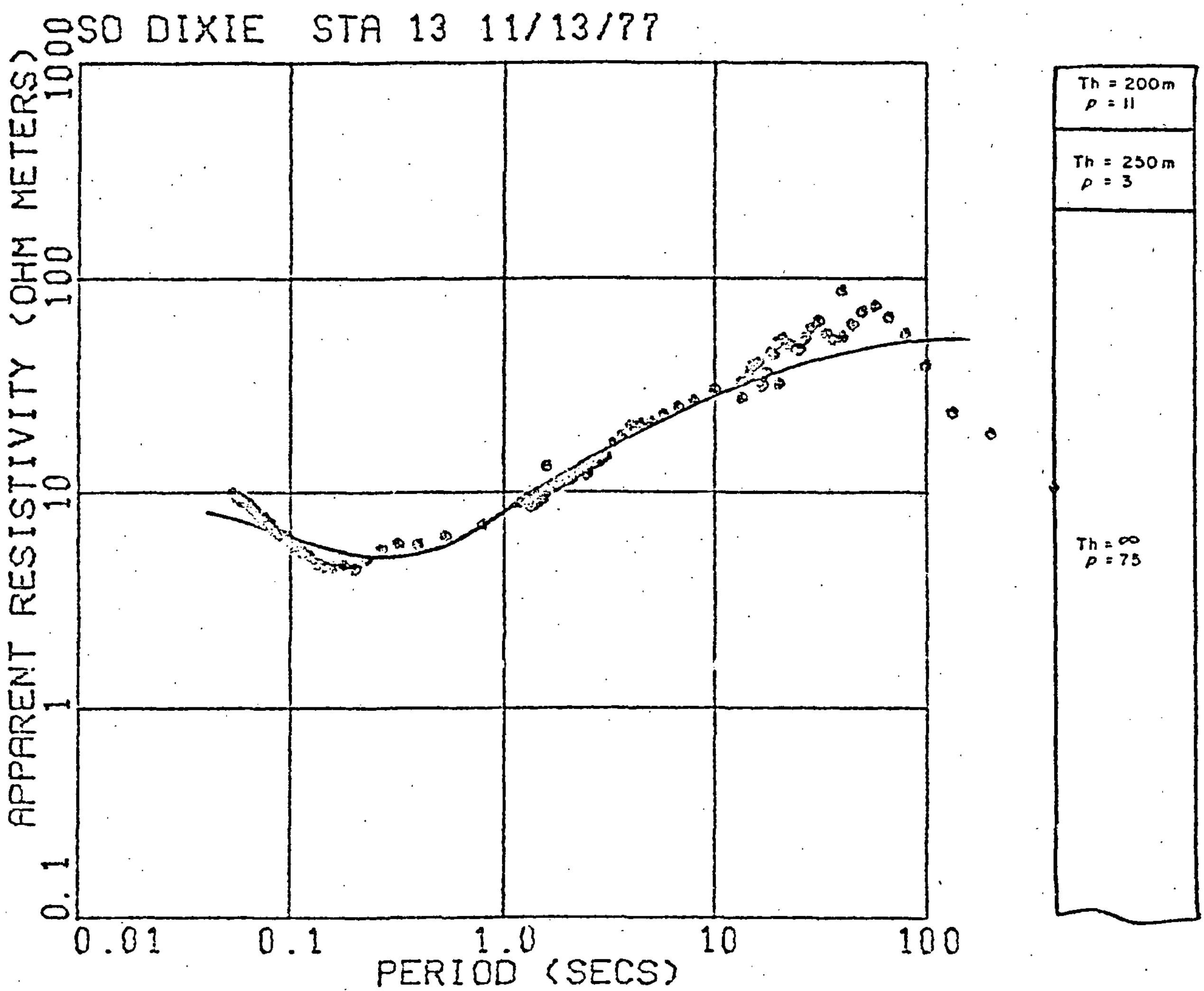
SO DIXIE STA 13 11/13/77
APPARENT RESISTIVITY (OHM METERS)
1000
100
10
1
0.1
0.01
0.1
1.0
10
100
PERIOD (SECS)
Th = 200m
ρ = 11
Th = 250m
ρ = 3
Th = ∞
ρ = 75

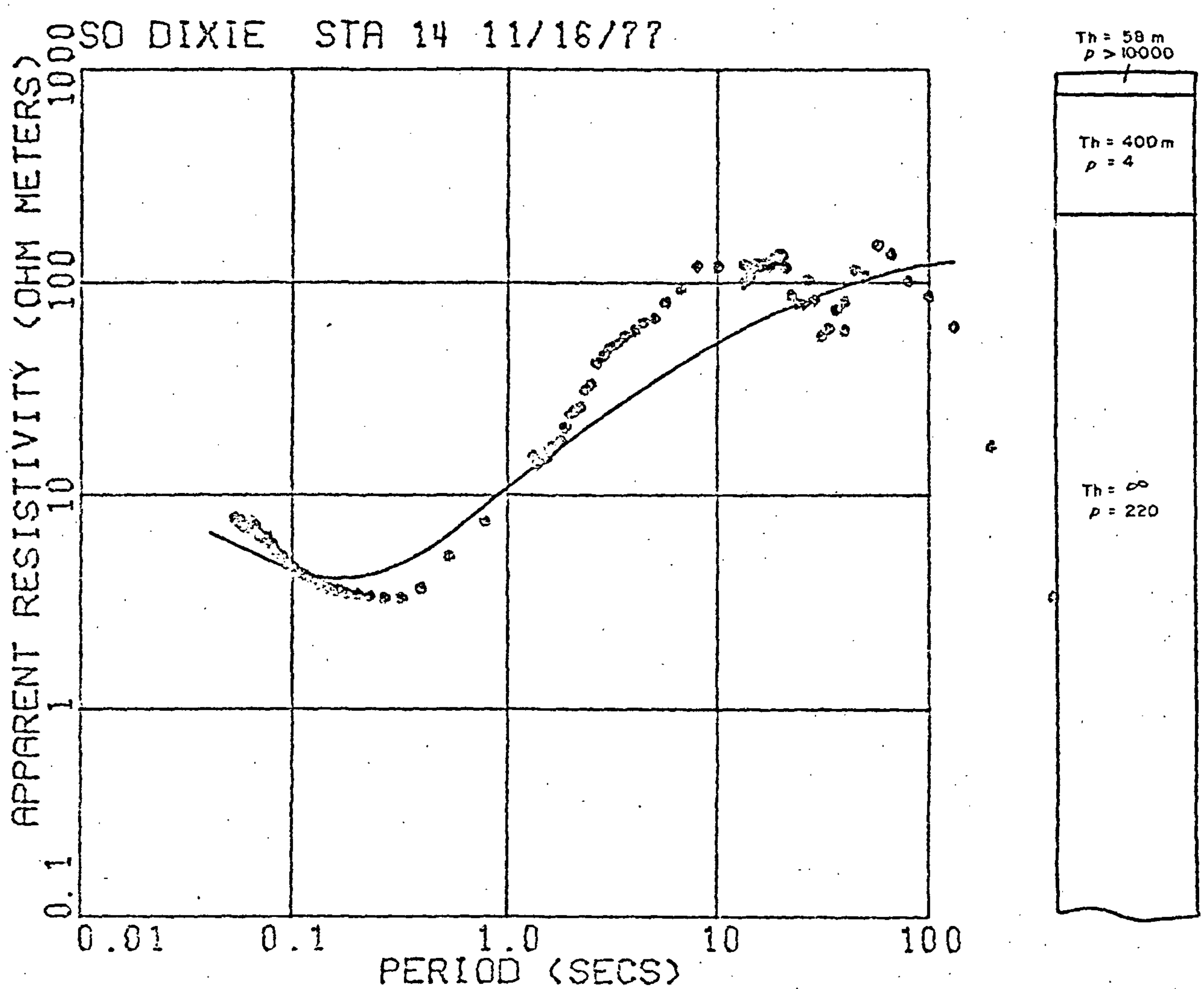
SO DIXIE STA 14 11/16/77
APPARENT RESISTIVITY (OHM METERS)
1000
100
10
1
0.1
0.01
0.1
1.0
10
100
PERIOD (SECS)
Th = 58 m
ρ > 10000
Th = 400 m
ρ = 4
Th = ∞
ρ = 220

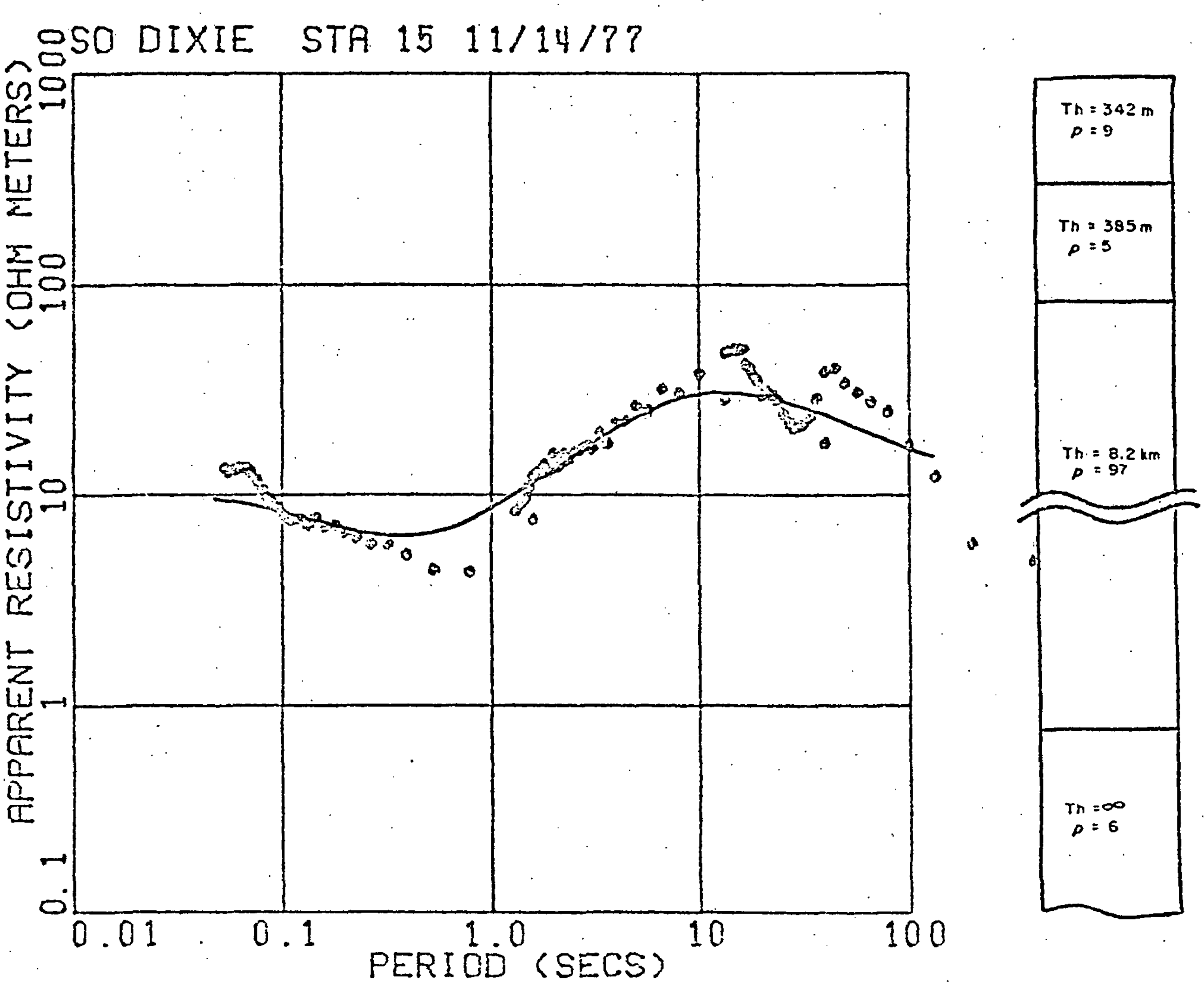

SO DIXIE STA 15 11/14/77
APPARENT RESISTIVITY (OHM METERS)
1000
100
10
1
0.1
0.01
0.1
1.0
10
100
PERIOD (SECS)
Th = 342 m
ρ = 9
Th = 385 m
ρ = 5
Th = 8.2 km
ρ = 97
Th = ∞
ρ = 6

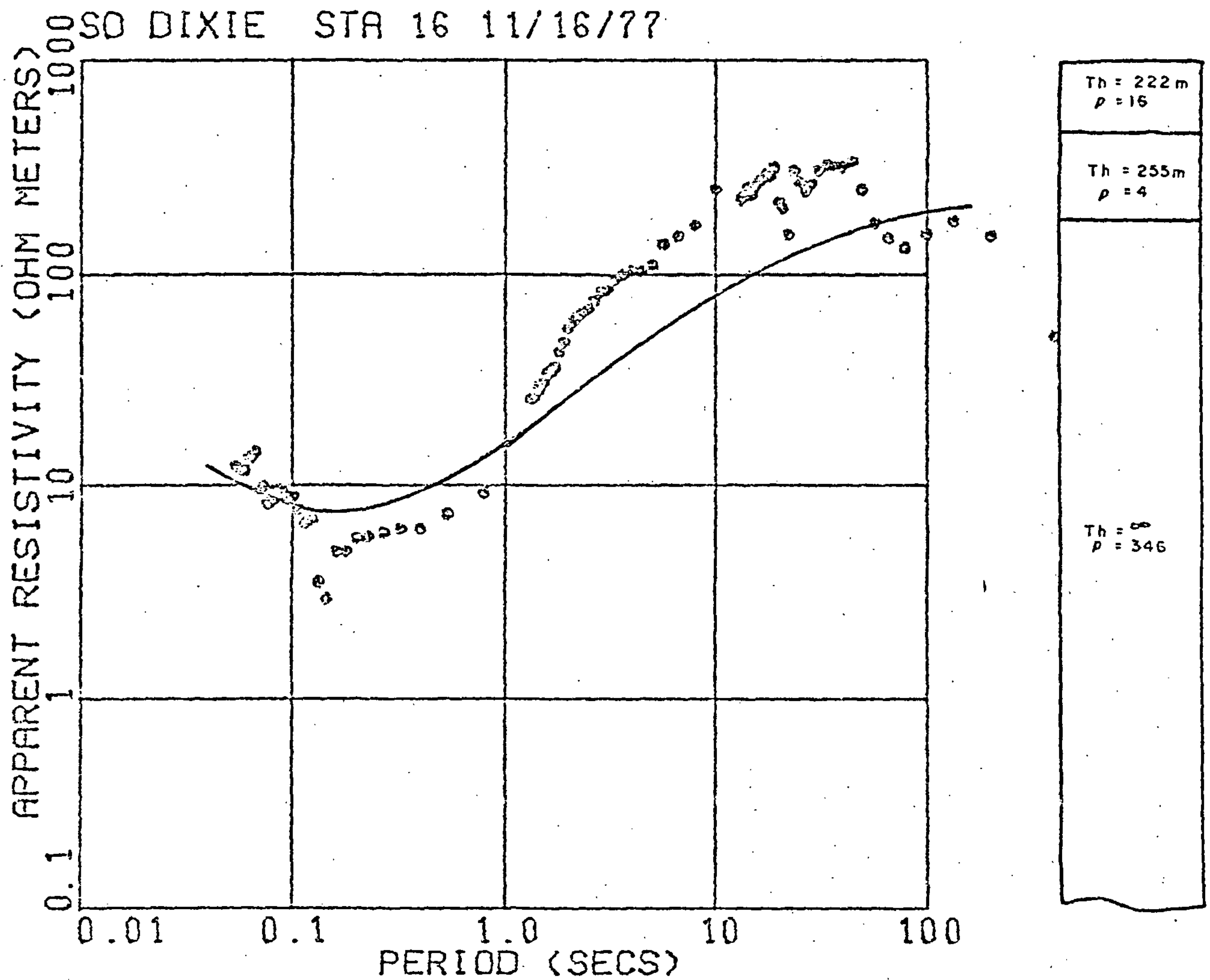
SO DIXIE STA 16 11/16/77
APPARENT RESISTIVITY (OHM METERS)
1000
100
10
1
0.1
0.01
0.1
1.0
10
100
PERIOD (SECS)
Th = 222m
ρ = 16
Th = 255m
ρ = 4
Th = ∞
ρ = 346

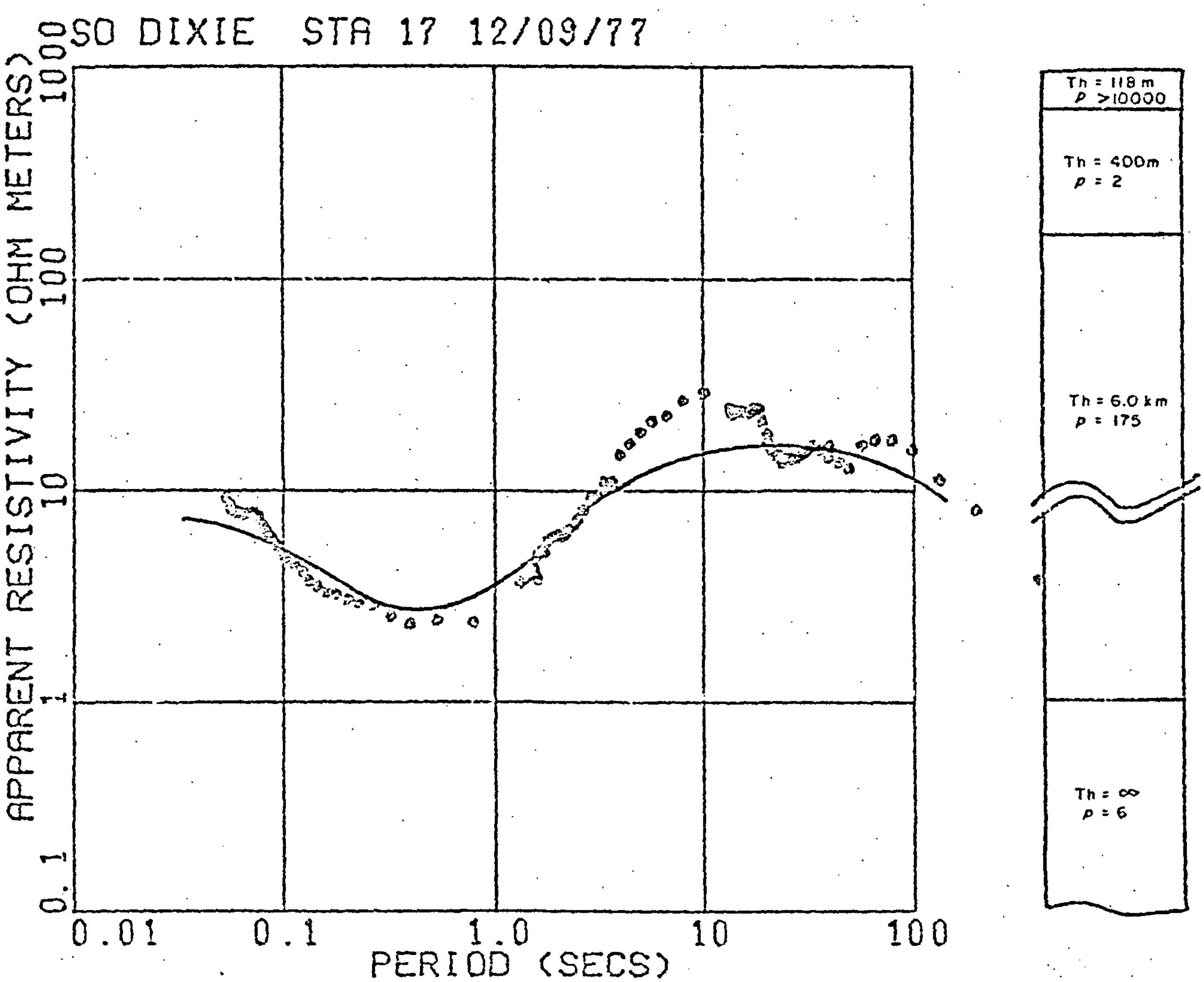

SO DIXIE STA 17 12/09/77
APPARENT RESISTIVITY (OHM METERS)
1000
100
10
1
0.1
0.01
0.1
1.0
10
100
PERIOD (SECS)
Th = 118 m
ρ >10000
Th = 400m
ρ = 2
Th = 6.0 km
ρ = 175
Th = ∞
ρ = 6

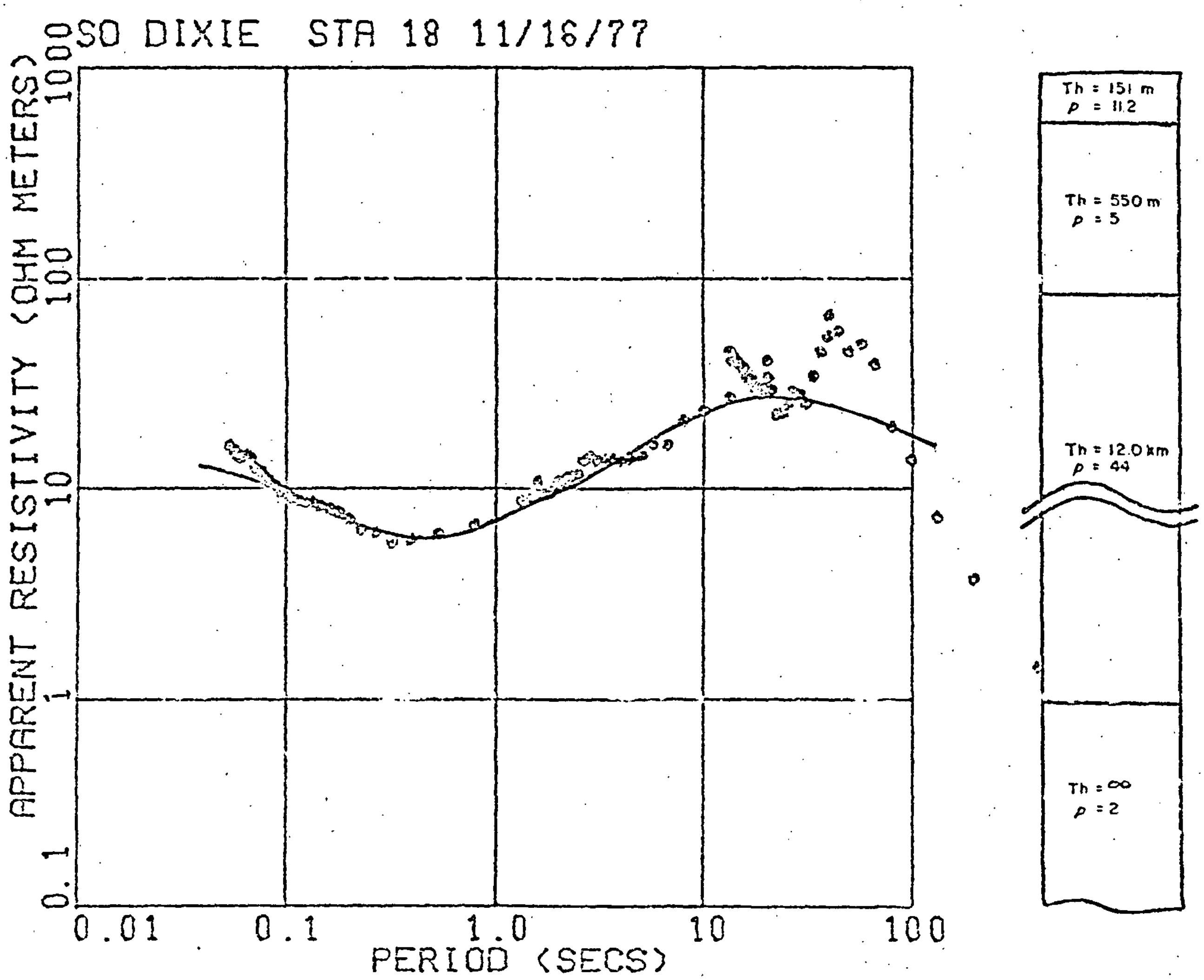
SO DIXIE STA 18 11/16/77
APPARENT RESISTIVITY (OHM METERS)
1000
100
10
1
0.1
0.01
0.1
1.0
10
100
PERIOD (SECS)
Th = 151 m
ρ = 11.2
Th = 550 m
ρ = 5
Th = 12.0 km
ρ = 44
Th = ∞
ρ = 2

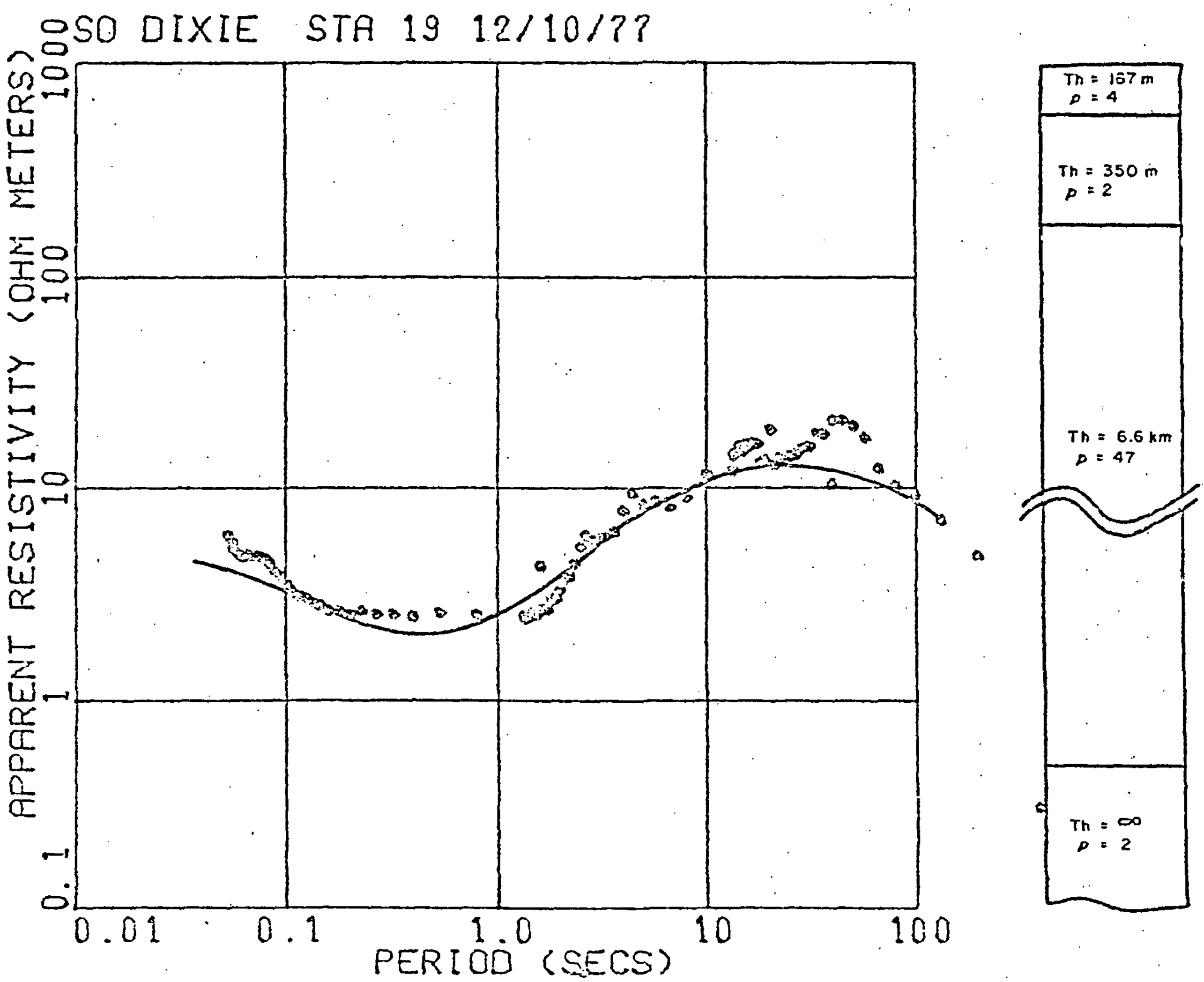

SO DIXIE STA 19 12/10/77
APPARENT RESISTIVITY (OHM METERS)
1000
100
10
1
0.1
0.01
0.1
1.0
10
100
PERIOD (SECS)
Th = 167 m
ρ = 4
Th = 350 m
ρ = 2
Th = 6.6 km
ρ = 47
Th = ∞
ρ = 2

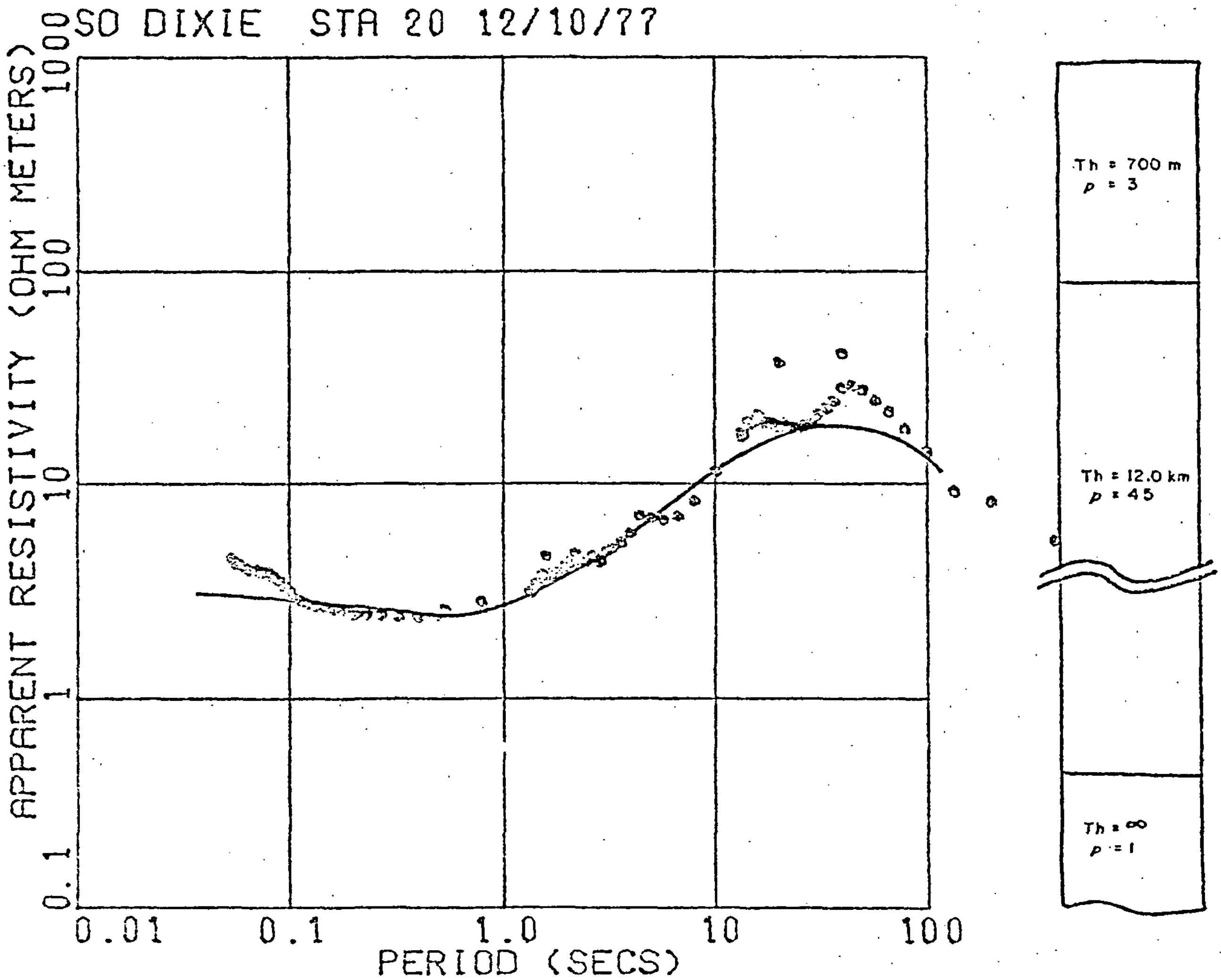
SO DIXIE STA 20 12/10/77
APPARENT RESISTIVITY (OHM METERS)
1000
100
10
1
0.1
0.01
0.1
1.0
10
100
PERIOD (SECS)
Th = 700 m
ρ = 3
Th = 12.0 km
ρ = 45
Th = ∞
ρ = 1

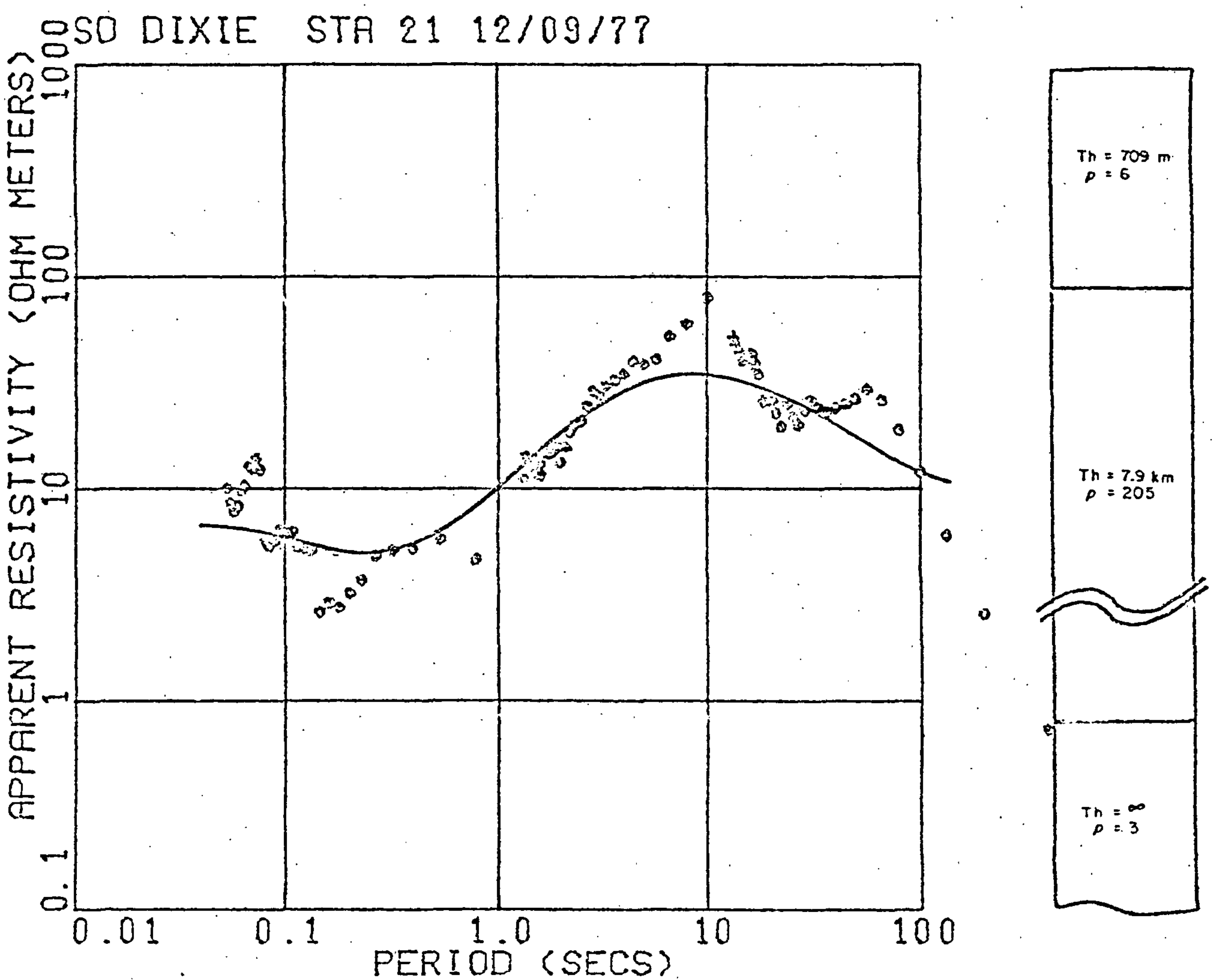
SO DIXIE STA 21 12/09/77
APPARENT RESISTIVITY (OHM METERS)
1000
100
10
1
0.1
0.01
0.1
1.0
10
100
PERIOD (SECS)
Th = 709 m
ρ = 6
Th = 7.9 km
ρ = 205
Th = ∞
ρ = 3

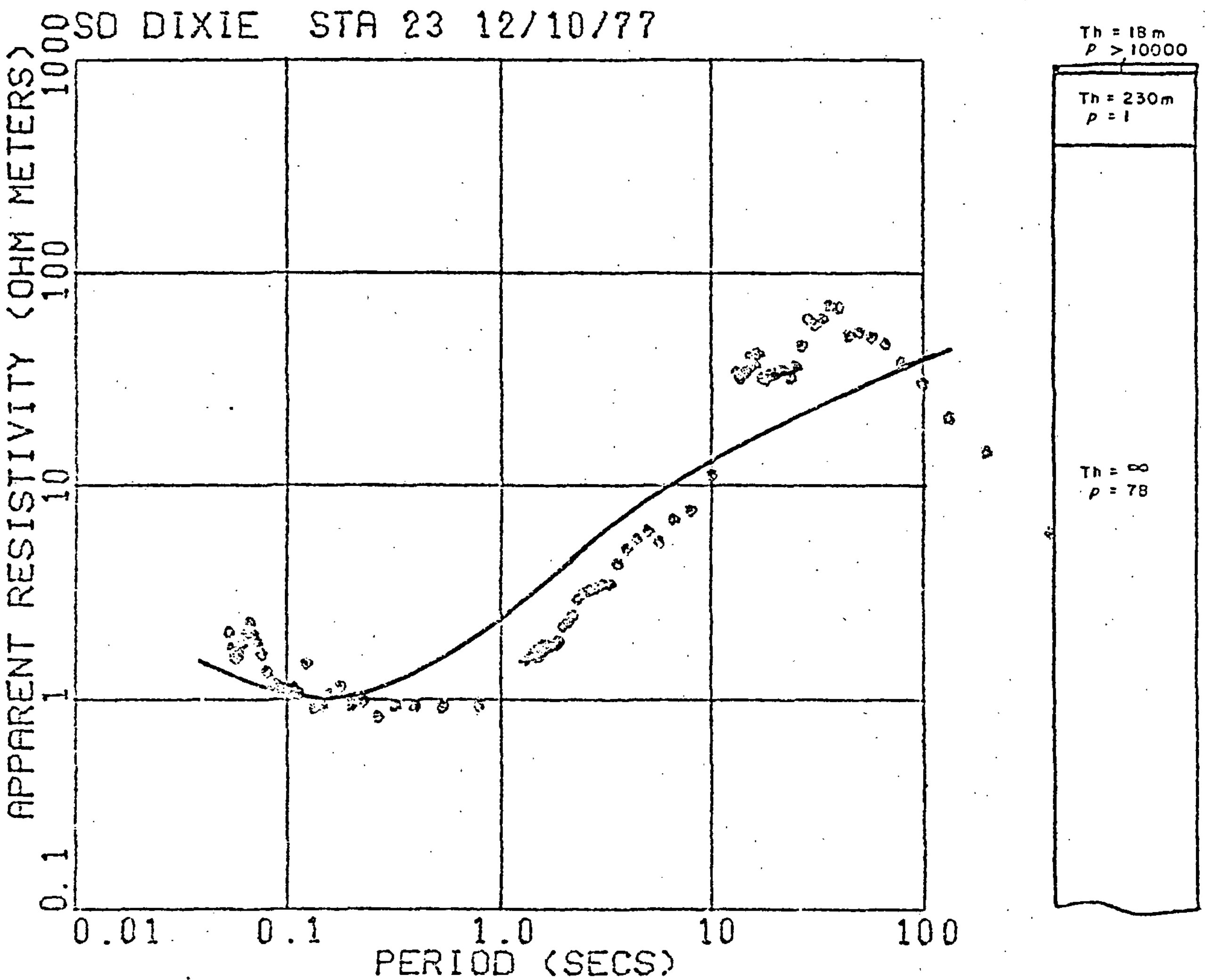
SO DIXIE STA 23 12/10/77
APPARENT RESISTIVITY (OHM METERS)
1000
100
10
1
0.1
0.01
0.1
1.0
10
100
PERIOD (SECS)
Th = 18 m
ρ > 10000
Th = 230m
ρ = 1
Th = ∞
ρ = 78

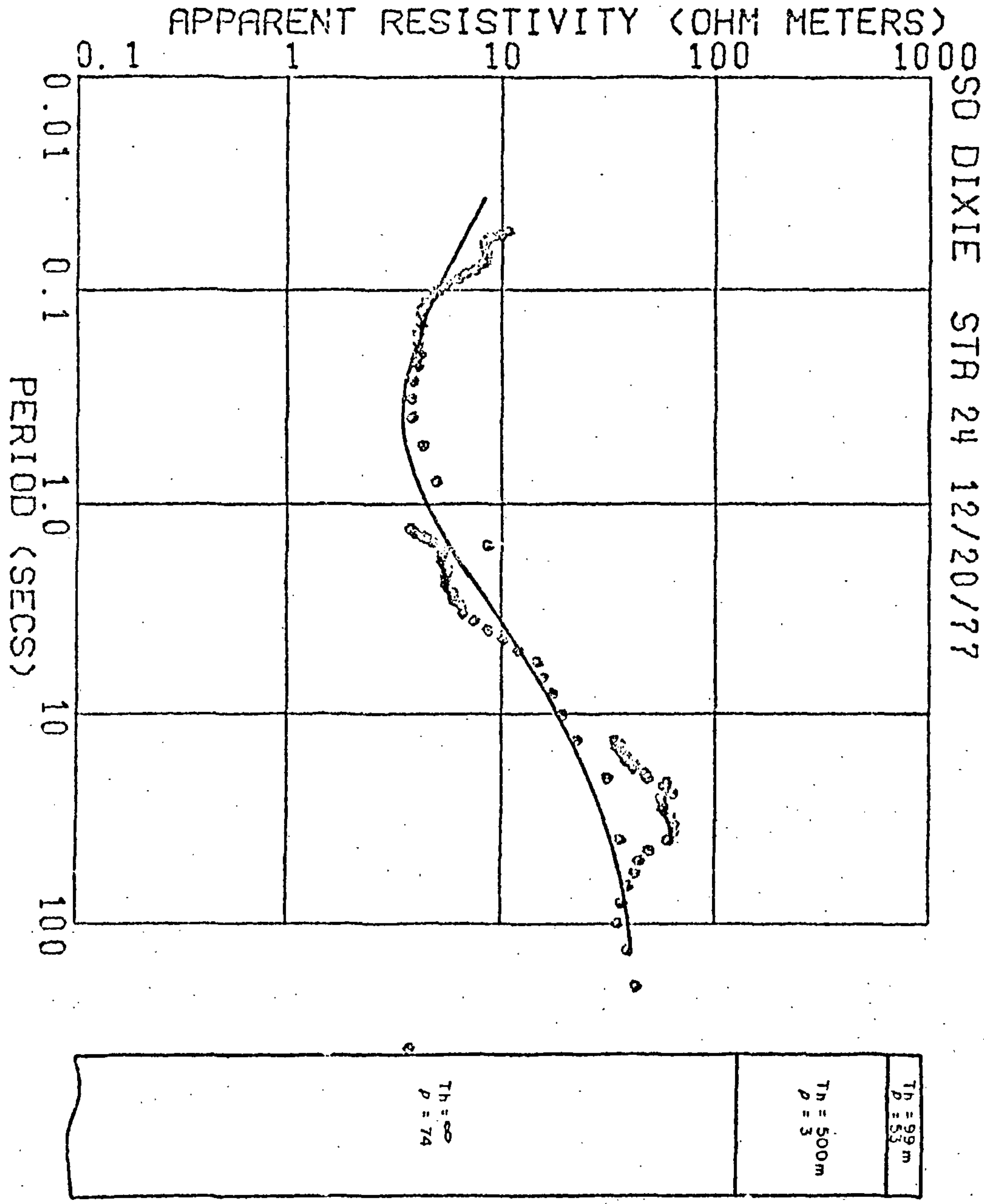
APPARENT RESISTIVITY (OHM METERS)
0.1
1
10
100
1000
0.01
0.1
1.0
10
100
PERIOD (SECS)
SD DIXIE STA 24 12/20/77
Th = ∞
ρ = 74
Th = 500m
ρ = 3
Th = 99m
ρ = 53

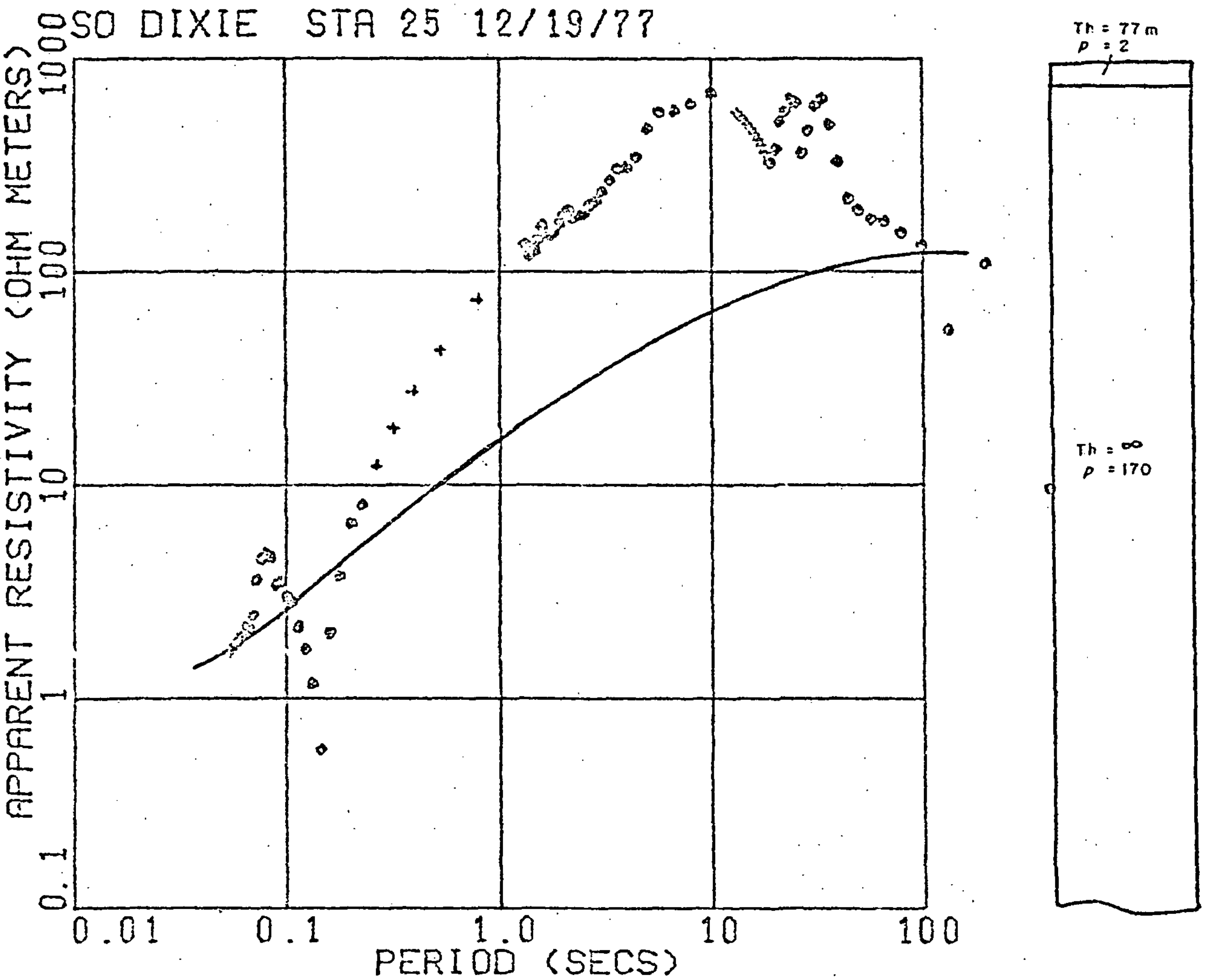

SO DIXIE STA 25 12/19/77
APPARENT RESISTIVITY (OHM METERS)
1000
100
10
1
0.1
0.01
0.1
1.0
10
100
PERIOD (SECS)
Th = 77 m
ρ = 2
Th = ∞
ρ = 170

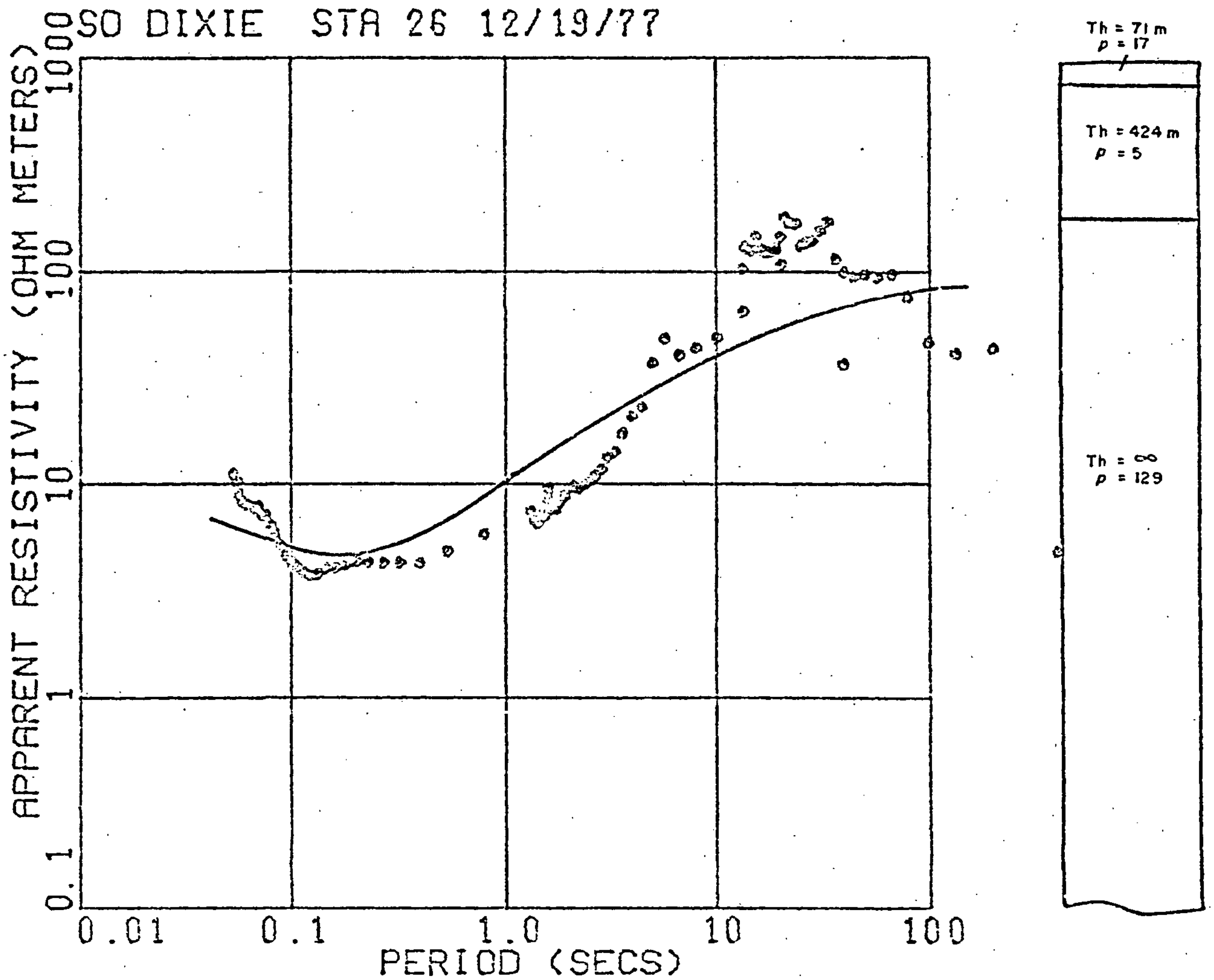
SO DIXIE STA 26 12/19/77
APPARENT RESISTIVITY (OHM METERS)
1000
100
10
1
0.1
0.01
0.1
1.0
10
100
PERIOD (SECS)
Th = 71 m
ρ = 17
Th = 424 m
ρ = 5
Th = ∞
ρ = 129

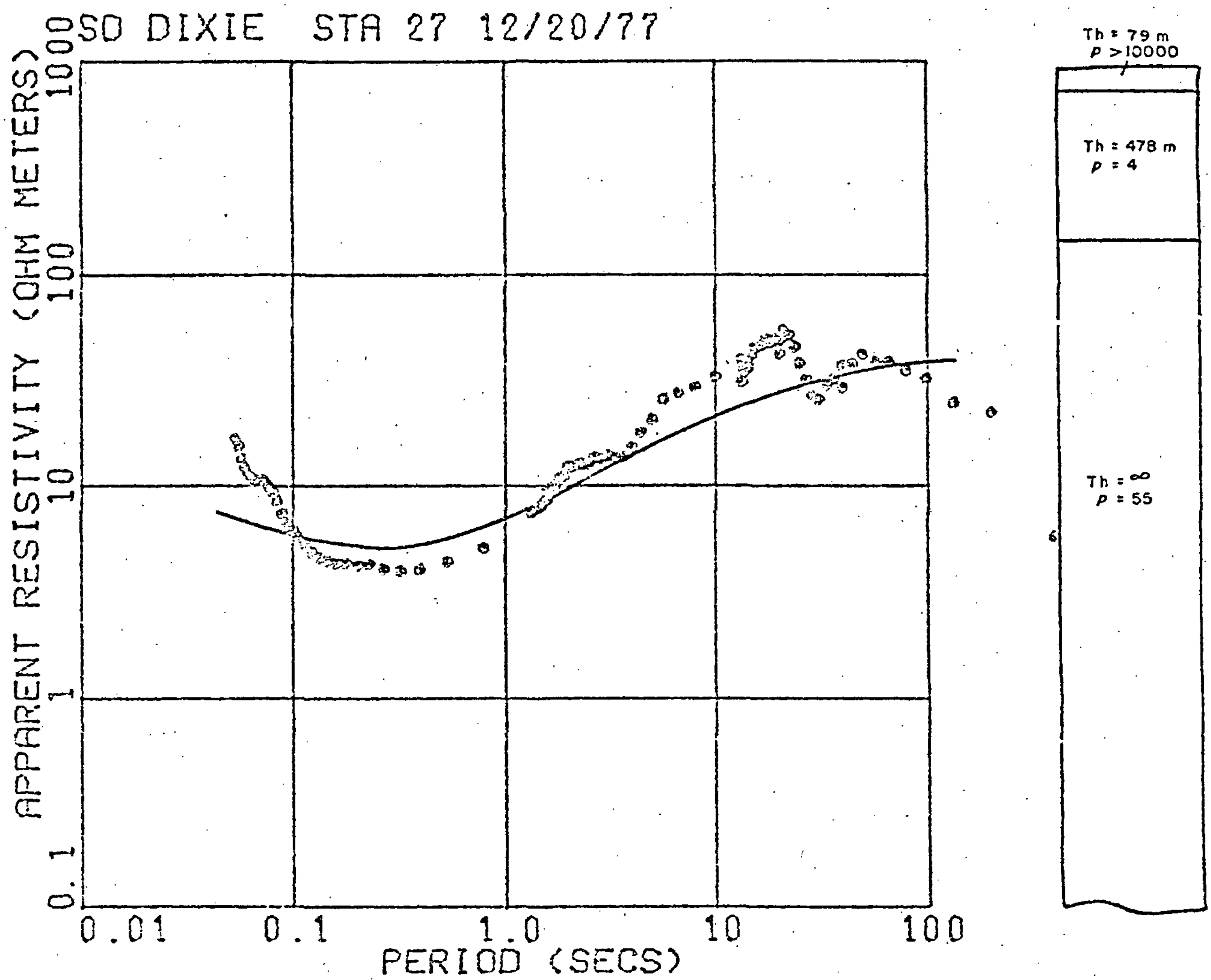
SO DIXIE STA 27 12/20/77
APPARENT RESISTIVITY (OHM METERS)
1000
100
10
1
0.1
0.01
0.1
1.0
10
100
PERIOD (SECS)
Th = 79 m
ρ >10000
Th = 478 m
ρ = 4
Th = ∞
ρ = 55

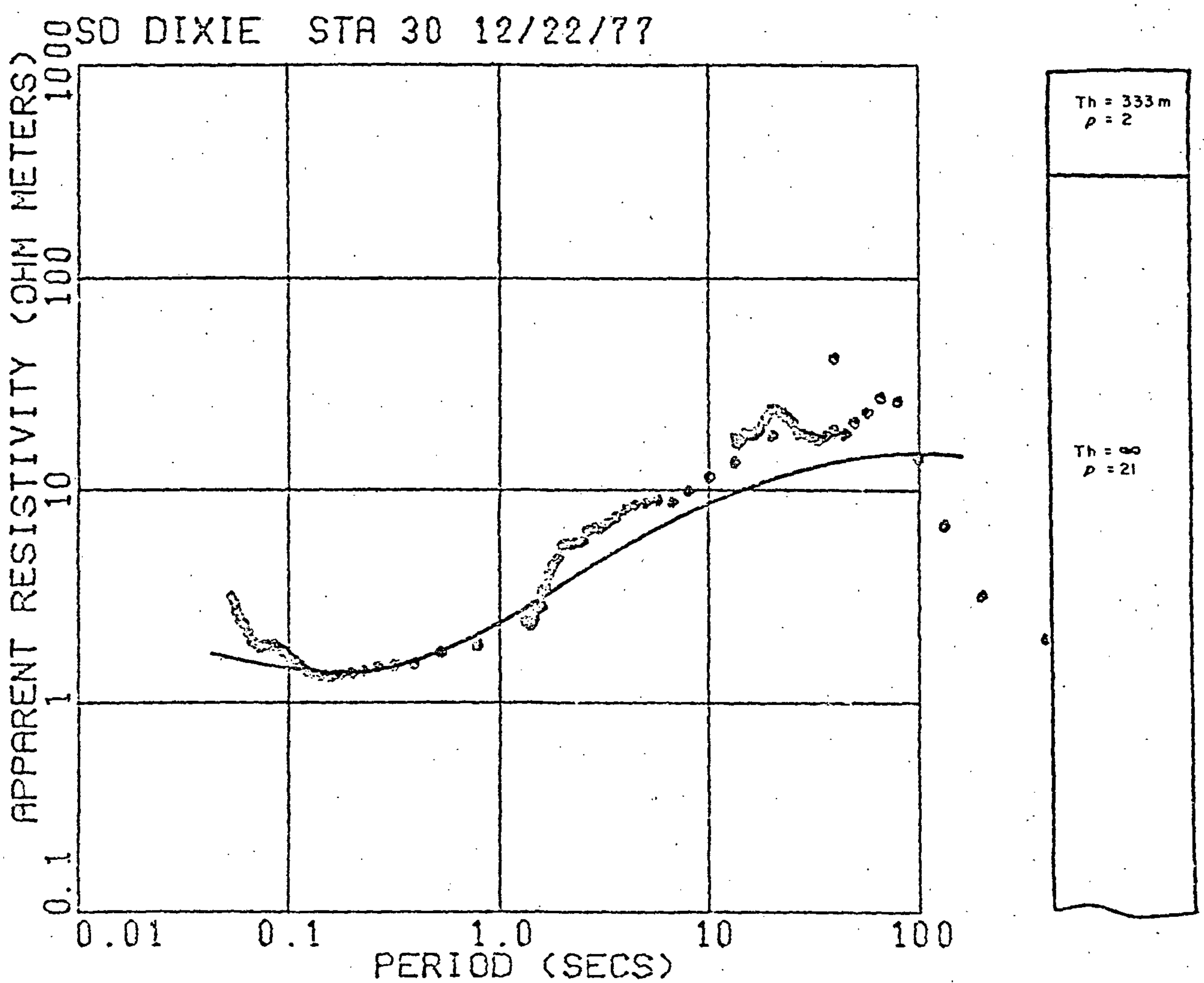

SO DIXIE STA 30 12/22/77
APPARENT RESISTIVITY (OHM METERS)
1000
100
10
1
0.1
0.01
0.1
1.0
10
100
PERIOD (SECS)
Th = 333 m
ρ = 2
Th = ∞
ρ = 21